Published in final edited form as:
Eur J Neurosci. 2012 December ; 36(12): 3615–3627. doi:10.1111/ejn.12002.

New Rules Governing Synaptic Plasticity In Core Nucleus Accumbens Medium Spiny Neurons

Xincai Ji and **Gilles E. Martin**
University of Massachusetts Medical School, The Brudnick Neuropsychiatric Research Institute, Department of Psychiatry; 303 Belmont Street, Worcester, MA 01604

Abstract

The nucleus accumbens is a forebrain region responsible for drug reward and goal directed behaviors. It has long been believed that drugs of abuse exert their addictive properties on behavior by altering the strength of synaptic communication over long periods of time. To date, attempts at understanding the relationship between drugs of abuse and synaptic plasticity have relied on the high-frequency long-term potentiation model of Bliss and LØmo (1973). We examined synaptic plasticity using spike-timing-dependent plasticity, a stimulation paradigm that reflects more closely *in vivo* firing patterns of core NAcc medium spiny neurons and their afferents. In contrast to other brain regions, the same stimulation paradigm evoked bidirectional long-term plasticity. Long-term potentiation (tLTP) magnitude changed with delay between action potentials (APs) and excitatory post-synaptic potentials (EPSPs), and frequency, while that of long-term depression (tLTD) remained unchanged. We showed that tLTP depended on NMDA receptors, whereas tLTD relied on action potentials. Importantly, intracellular calcium signaling pathways mobilized during tLTP and tLTD were different. Thus, calcium-induced calcium release underlies tLTD but not tLTP. Finally, we found that the firing pattern of a subset of MSNs was strongly inhibited by dopamine receptor agonists. Surprisingly, these neurons were exclusively associated with tLTP but not with tLTD. Taken together, these data point to the existence of two subgroups of MSNs with distinct properties, each displaying unique abilities to undergo synaptic plasticity.

Keywords

spike-timing-dependent plasticity; dopamine; calcium stores; endocannabinoids; whole-cell patch-clamp recording; mice

Introduction

The nucleus accumbens (NAcc) is a pivotal component of the brain reward and addiction circuitry (Chen et al., 2010). There is solid evidence that alteration of neuronal plasticity by drugs of abuse is a conduit for their addictive properties (Hyman et al., 2006; Kauer and Malenka, 2007). To date, actions of drugs of abuse on synaptic plasticity have been examined using high-frequency stimulation long-term potentiation (HFS-LTP), the canonical model developed by Bliss and Lømo (1973). Although this model has proven useful, it presents one major limitation with regard to NAcc. Indeed, HFS-LTP is found in

Corresponding author: Gilles E. Martin, University of Massachusetts Medical School, The Brudnick Neuropsychiatric Research Institute, Department of Psychiatry; 303 Belmont Street, Worcester, MA 01604. Tel: 508 856-4074, Fax: 508 856-2526, gilles.martin@umassmed.edu.

The authors have no competing interests.

less than 20% of MSNs (Kombian and Malenka, 1994; Robbe et al., 2002a; Schramm et al., 2002). This low induction rate raises the question of whether high-frequency stimulation (i.e., 100 Hz) pattern is appropriate for studying synaptic plasticity in a region where medium spiny neurons (MSNs), the main neuronal population, typically fire between 1 and 10 Hz in freely moving animals (Carelli and Ijames, 2000; Hollander et al., 2002; Krause et al., 2010). Moreover, MSNs receive glutamatergic inputs from the amygdala and prefrontal cortex whose neurons also fire at similarly low frequencies (Rosenkranz and Grace, 1999; Margrie et al., 2002; Puig et al., 2003). We addressed this limitation by using the spike timing dependent plasticity model (STDP; (Markram et al., 1997)). We elicited both tLTP and tLTD by pairing action potentials (APs) and excitatory postsynaptic potentials (EPSPs) at low *in vivo*-like frequencies (i.e., 0.2, 1, and 5 Hz). We found that, unlike other brain regions (e.g. hippocampus and cortex), all APs-EPSPs pairing protocols evoke both tLTP and tLTD. Whereas amplitude of tLTP varies with pairing frequencies and delays between EPSPs and APs, that of tLTD is insensitive to these parameters and remains constant regardless of experimental conditions. Blockade of APs, or alterations of their properties in BK channel β1 knockout mice, suppress tLTD but not tLTP, whereas inhibition of NMDA receptors blocks tLTP but leaves tLTD intact. Antagonizing high-threshold L-type calcium channels and calcium-induced calcium release (CICR) through ryanodine receptors nearly totally blocked tLTD but had no effect on tLTP. Finally, whereas dopamine D1 and D2 receptor agonists have no effect on firing pattern of LTD-MSNs, they totally inhibit that of tLTP-MSNs. Taken together; our data indicate that under similar experimental conditions, accumbens spiny neurons can be divided in two subgroups (i.e., tLTP and tLTD) with different characteristics.

Methods

All animal procedures were conducted in accordance with the National Institutes of Health's Guide for the Care and Use of Laboratory Animals and with protocols approved by the Institutional Animal Care and Use Committee of the University of Massachusetts Medical School. Mice were housed four per cage and maintained at constant temperature and humidity with a 12-h light–dark cycle. Water and food were provided ad libitum.

Animals and slice preparation

We used 21–30 days old male C57BL/6 mice to prepare slices from fresh brain tissue. Mice were deeply anesthetized with isoflurane, and killed by decapitation. We rapidly removed and transferred the brain in a cold (~ +0.5°C) oxygenated (95% O_2 and 5% CO_2) high-sucrose solution of the following composition (in mM): 125 Sucrose, 53 NaCl, 2.5 KCl, 1.25 NaH_2PO_4, 1 $MgCl_2$, 2 $CaCl_2$, 25 D-Glucose, 26 $NaHCO_3$, and kynurenic acid (0.18 mg/ml). We cut slices (300 μm) transversely with a Vibroslicer (VT1200, Leica MicroInstrutments; Germany), and immediately transferred them in an incubation chamber containing a modified Earl's Balance Salt Solution (EBSS) maintained at 35° C. Slices were left to recuperate in the EBSS solution for 50 min to 1 hour before being moved into an artificial cerebrospinal fluid (ACSF; in mM): 126 NaCl, 2.5 KCl, $NaH_2PO_4.H_2O$, 1 $MgCl_2$, 2 $CaCl_2$, 26 $NaHCO_3$, 25 D-Glucose, at room temperature. We submerged and perfused slices at room temperature (~21°C) with a carbogenated ACSF, at a constant rate of 1 – 2 ml /min. We visualized neurons in infrared differential interference contrast (IR-DIC) videomicroscopy using a fully motorized microscope (Scientifica; Uckfield England) mounted with Olympus objectives (10 and 60x; Olympus Microscopy, Japan) and condenser.

Electrophysiology

We filled borosilicate glass electrodes (1.5 mm OD, 4–6 MΩ resistance) with an internal solution containing (mM): 120 K-methanesulfonate; 20 KCl; 10 Hepes; 2 K2ATP, 2 K_2GTP, and 12 phosphocreatine. We acquired voltage and current traces in whole-cell patch-clamp recording mode from core MSNs using an EPC10 double amplifier (HEKA Elektronik; Germany). We analyzed traces with FitMaster 2.15 software package (HEKA Elektronik; Germany). We sampled and filtered current and voltage traces at 20 kHz, and 2 kHz respectively. We monitored input resistance (Rin) throughout recording sessions. We rejected recordings with changes larger than 20%.

To evoke synaptic events, we positioned a bipolar stimulation electrode (FHC; Bowdoin, ME) ventral of the anterior commissure, at the interface between core and shell accumbens regions. In control (10 min) and post-induction (up to 70 min) conditions, we evoked EPSPs at 0.05 Hz at resting membrane potential (RMP ~ −88 mV; the junction potential was left uncompensated). We adjusted the stimulus intensity (100 μs, 40–100 *m*A) to evoke subthreshold EPSPs between +5 and +15 mV amplitude. We generated tLTP and tLTD by pairing an EPSP and a postsynaptic AP evoked with a 5 ms/800 pA depolarizing pulse. We tested several delays (10, 20, 50 and 200 ms) separating these two electrical events at various frequencies (0.2, 1, and 5 Hz) as shown in the matrix of experimental conditions (Table 1). When APs preceded EPSPs, delays between the two electrical events were assigned a positive sign. When they followed EPSPs, delays were assigned a negative sign. We also recorded 100 sec gap-free spontaneous EPSCs activity (sEPSCs) at resting membrane potential following a 10 min control period and 15 to 20 min after induction of plasticity in order to associate changes of sEPSCs amplitude and frequency with tLTP/tLTD. MSNs with sEPSCs frequency lower than 1 Hz were not included in the analysis. sEPSCs, acquired at 20 kHz and filtered at 1 kHz, were analyzed with Mini 6.0 software (Synaptosoft Inc, GA, USA). The threshold was determined by the formula √rms×3 (~ 6 – 7 pA). We monitored series resistance by comparing EPSCs decay time before and after induction.

To study action of dopamine receptor agonists on MSNs resting membrane potential (RMP), Rin, and firing pattern, we injected one hyperpolarizing (−110 pA, 800 ms) and depolarizing (~+260 pA but adjusted to evoke about 7–8 APs) current steps 10 sec apart. This protocol, applied every 30 sec before and during exposure to drugs, followed our usual plasticity stimulation paradigm (10 min control, AP-EPSP 20 ms 1 Hz, 10 min post induction period) to determine whether the recorded cell was “tLTP” or “tLTD”.

Analysis

We compared EPSPs maximum amplitude measured in a 20 ms time window, 10 ms after the stimulus artifact, with its baseline amplitude 10 ms before it. We performed this measurement on 30 consecutive EPSPs before, and 20 min after APs-EPSPs pairing. We expressed the difference of EPSP amplitude before and after induction as percent of control (100 %). EPSP inactivation rate was measured by fitting the decay of the voltage from the EPSP maximum amplitude point to a steady voltage about 200 ms after using a single exponential. We monitored membrane input resistance and electrode series resistance throughout the recording session by injecting every 20 sec a short (250 ms) hyperpolarizing current pulse (−20 pA) following each EPSPs. We measured APs width, fast afterhyperpolarization (fAHP), overshoot and threshold. Width was measured at potential half way between AP threshold and maximum amplitude. We defined fAHP and overshoot as the minimum value during the repolarization phase following each AP, and the maximum depolarization measured from a threshold (0 mV), respectively. Threshold was the point of inflection when depolarization abruptly increases before reaching its maximum amplitude. Data were analyzed by using Student’s one sample or unpaired t tests, with $P < 0.05$

considered statistically significant. We evaluated sEPSCs frequency and amplitude by using cumulative probability analysis, and statistical significance was determined by using the Kolmogorov–Smirnov, nonparametric, two-sample test (Van der Kloot, 1991), with $P < 0.05$ considered significant. All results are expressed as mean ± SEM values. We performed statistical analysis in STDP experiments using Prism 5 (Graphpad, CA, USA) running on a Mac Power PC G5.

Bicuculline, and ifenprodil, were purchased from Sigma-Aldrich (USA). A-77636, quinpirole, thapsigargine, nifedipine and ryanodine, as well as the endocannabinoid antagonist AM-251, were purchased from Tocris Bioscience (Bristol, UK). Tetrodotoxin (TTX) was purchased from Alomone Labs (Jerusalem, Israel).

Results

Influence of delay, frequency on plasticity

Given the well-documented influence of delay and frequency on STDP in a number of brain regions (Caporale and Dan, 2008), we first examined the effects of these parameters, and that of pairing order (i.e., AP preceding or following EPSP), on NAcc EPSP amplitude measured 30 min after induction. Surprisingly, all protocols, regardless of frequency, delay or pairing order, evoked invariably both tLTP and tLTD. Figure 1A and B shows a representative example of tLTP evoked by AP-EPSPs pairing at 1 Hz with a 10 ms interval. Sustained increase of EPSP amplitude (tLTP) was accompanied by stable input resistance (Fig. 1A, middle panel) and resting membrane potential (RMP; Fig. 1A bottom panel). In another MSN, the same pairing conditions evoked a robust depression (Fig. 1C and D). Increasing delay to 20 ms enhanced tLTP amplitude (Fig. 1E and F) while tLTD remained the same (Fig. 1G and H). Interestingly, the pattern of tLTP was similar at all pairing frequencies, with an optimal time window of 20 ms (Fig 1I, faded yellow vertical bar). Shorter (10 ms) and longer intervals (50 and 200 ms) displayed weaker tLTP (Fig. 1I; green line). In sharp contrast to previous findings from hippocampus, cortex, striatum and other brain regions (Sjostrom et al., 2008), the magnitude of tLTD remained surprisingly stable (75–85 % of control) for all (23) but one (i.e., EPSP-AP, 1 Hz, 50 ms) conditions tested (Fig. 1I and Table 1). As a whole, we found tLTD in slightly more MSNs (54%; 162 out of 299 neurons), although tLTP/tLTD ratio varied with conditions without clear pattern (Table 1). Rin and RMP were similar between tLTP (242 ± 18.06 MΩ, −88.2 ± 2.1 mV; n = 49) and tLTD (244.3 ± 10.51 MΩ, −89.3 ± 1.8 mV; n = 50) MSNs. Importantly, evoking EPSPs every 20 sec over a 35 min period in absence of any AP-EPSP pairing demonstrates that tLTP and tLTD are not caused by steady unidirectional (e.g., run-up) changes of synaptic strength over time (Suppl. Fig. 1). Although our decision to not block GABA-mediated synaptic transmission, in order to mimic as closely as possible conditions found in freely moving animals, could have introduced a confounding factor, we report that this is not the case. Indeed, we found no change of plasticity in presence of 15 μM bicuculline, a specific $GABA_A$ receptor antagonist (Fig. 2).

NMDA receptors and action potentials control tLTP and tLTD, respectively

NMDA receptors play a central role in conventional HFS-LTP (Bliss and Collingridge, 1993), and STDP (Markram et al., 1997; Bi and Poo, 1998). To investigate their contribution to core NAcc STDP, we exposed slices to 50 μM d-APV, a widely used NMDA receptor antagonist. After pairing (AP − EPSPs, 1 Hz, 20 ms delay), EPSP amplitude was potentiated in only 1 MSNs whereas tLTD was found in the remaining 12 MSNs (Fig. 3A, open squares), indicative of a strong shift in the ratio of tLTP/tLTD compared to conditions without d-APV (w/o d-APV; Fig. 2A). Averaged tLTD amplitude was similar (Fig. 3B), with (76.6 ± 4.5% of control; open square) or without d-APV (83.2 ± 4% of control, open

circle). Figure 3C shows a robust tLTD 20 min after plasticity induction from a representative MSN. We further explored the role of NMDA receptors by exposing slices to 10 μM ifenprodil, a specific antagonist for NMDA receptors containing the NR2B auxiliary subunit. This subunit, highly expressed in NAcc, has been linked to drugs of abuse reward and dependence (Yaka et al., 2003). Ifenprodil totally blocked tLTP but left the magnitude of tLTD unchanged (85.2 ± 3.7 % of control; Fig. 3D solid circle).

If these data unequivocally support the role of NMDA receptors in tLTP, they are at odds with previous findings indicating that NAcc conventional LTD is also NMDA receptor-dependent (Thomas et al., 2000). This raised the question of the mechanisms controlling tLTD. We addressed this issue by pairing subthreshold depolarizations (no AP was evoked with a brief 5 ms/500 pA depolarizing current pulse) with EPSPs (Fig. 4A) at 1 Hz with a 20 ms interval. In 7 out of 9 MSNs, tLTP amplitude ranged from 113 to 211 % of control (Fig. 4B, open circles), with an averaged value of 158.9 ± 11% (Fig. 4B, solid square), similar to that of control conditions (Fig. 4B, open square). In the remaining two cells, tLTD was weak. This dependence of tLTD on APs runs counter to findings by Fino et al (2009) in dorsal striatum where they recorded a robust tLTD in similar experimental conditions. Increasing the duration of the current pulse to 20 ms to evoke a subthreshold depolarization preceding EPSPs during induction produced similar results (Fig. 4C). We asked what would happen if we simply increased stimulation frequency from 0.05 (control) to 1 Hz (induction) in absence of any pairing (no current was injected before evoking EPSPs). Surprisingly, a total lack of APs/subthreshold depolarization prevented tLTD but not tLTP formation (Fig. 4D), indicating that the latter occurred simply when EPSPs frequency increases slightly. Having shown that tLTD depended tightly on APs, we examined the degree of this dependence. Thus, instead of bluntly suppressing APs, we manipulated their properties using voltage- and calcium-gated high conductance potassium channels (BKs). These channels, activated by the cooperative effects of membrane depolarization and cytoplasmic Ca^{2+}, form large macromolecular complexes with high threshold voltage-gated calcium channels (VGCC) (Marrion and Tavalin, 1998), the main calcium entryways during APs-driven depolarization (Poolos and Johnston, 1999; Miranda et al., 2003). As such, BK channels control action potentials repolarization and AHP (Shao et al., 1999, #55070; Poolos and Johnston, 1999; Matthews et al., 2008). Instead of totally blocking BK channels (e.g. using a BK α subunit KO) we altered its function (see Behrens et al., 2000), and by extension APs properties during induction of plasticity (Suppl. Fig. 4E and F), using mice lacking BK channel β1 auxiliary subunit expressed in core NAcc (Martin et al., 2004). Alterations of APs properties in KO mice did not block tLTP (Fig. 5A), whose averaged amplitude (158.6 ± 10.3 % of control) matched that of wt mice (Fig. 5B), but prevented tLTD (Fig. 5B). We obtained a similar result by exposing MSNs to 1 μM Iberiotoxin (IbTx), a specific αβ1 BK channel antagonist (Fig. 5C). Because a concomitant change of EPSP kinetics may cloud the interpretation, we compared EPSPs decay rate in wt and β1 KO mice. We showed that EPSP deactivation in wt and β1 mice was 23 ± 1.01 and 23 ± 1.05 ms, respectively (Fig. 5E), indicating that the lack of tLTD in KO mice could not be attributed to a change in EPSP kinetics.

In light of the pivotal role of APs in tLTD, we asked whether its locus of action was presynaptic as suggested by recent studies (Robbe et al., 2002b; Grueter et al., 2010). Indeed, the lack of dependence of tLTD on frequency seemingly argued against the release of endocannabinoids/adenosine, transmitters commonly associated with a presynaptic tLTD (Robbe et al., 2001; Robbe et al., 2002b). We recorded spontaneous, not mini EPSCs. Indeed, APs amplitude never fully recovered after washing off TTX (0.25 μM) from the recording chamber (we needed to apply TTX twice, before and after induction; n = 3, Suppl. Fig. 3), which prevented tLTD induction, further supporting the pivotal role of APs on tLTD. As a control, we found that both sEPSCs amplitude (~15 – 20 pA) and frequency (~ 2

Hz) were stable in control conditions when no pairing was used (Suppl. Fig. 4). In tLTP MSNs, a representative example shown in Fig. 6A reveals that EPSCs amplitude increased (Fig. 6A), but its frequency, a feature confirmed when amplitude and frequency distribution were averaged over 4 MSNs (Fig. 6B). In contrast, In MSNs where AP-EPSP pairing induced tLTD, amplitude remained unchanged (Fig. 6C left panel) while frequency significantly decreased ($F_{1, 6} = 48.20$, $p = 0.034$) 20 min after induction, a shift that was significant when averaged over 6 MSNs ($F_{1, 10} = 84.25$, $p = 0.014$; Fig. 6D; right panel). These data support the idea that tLTD is a presynaptic phenomenon, while tLTP relies on a postsynaptic mechanism, and is in line with previous findings in NAcc (Robbe et al., 2003). It is widely believed that the release of endocannabinoids by NAcc MSNs is responsible for LTD. To examine this possibility, we blocked cannabinoid receptors (CB1) with 2 μM AM-251, as they are presynaptically expressed on glutamatergic terminals. Exposure of slices to this antagonist totally blocked tLTD while leaving tLTP intact (Fig. 7).

tLTP and tLTD recruit different calcium signaling pathways

Although our data support the idea that tLTP and tLTD stem from activation of different cellular pathways, this does not fully answer a seemingly paradoxical result. What is the mechanism that decides whether a MSN undergoes tLTP or tLTD considering that both are evoked in similar conditions (AP-EPSP, 20 ms 1 Hz), and have the same endpoint i.e., modulation of AMPA receptors? One possible answer may hinge on calcium dynamics. Although tLTP and tLTD presumably both rely on calcium influx through NMDA receptors and calcium channels activated during APs-driven depolarization, it is unclear whether pools of intracellular calcium mobilized during these two forms of plasticity are the same. We explored this question by inhibiting high threshold L-type calcium channels with 5 μM nifedipine. Because of their voltage dependence, we anticipated that they would be readily activated during APs, and much less during the comparatively small EPSP-driven depolarization. We found that nifedipine blocked tLTD, and slightly diminished tLTP magnitude to 132 ± 4.2 % of control (Fig. 8C) compared to conditions when the drug was not added to the recording pipette solution (147.8 ± 15.5 % of control), although the difference was not statistically significant ($p = 0.14$). We then asked whether this calcium influx mobilized calcium from intracellular calcium stores. To test this possibility, we blocked CICR with 10 μM ryanodine in the recording pipette. Similarly, ryanodine blocked tLTD while tLTP could readily be evoked (Fig. 8A right panel, and 8C). Finally, we further probed the role of intracellular calcium stores by depleting them from calcium with 5 μM thapsigargine. Again, this drug abolished tLTD without noticeably affecting tLTP (Fig. 8A left panel, and 8C). These data support the idea that in a subset of MSNs, L-type calcium channels are presumably in close proximity with ryanodine receptors, and the resulting increase of intracellular calcium concentration leads to tLTD but not tLTP. None of these drugs' actions on tLTP were significantly different than in control conditions. Having shown that CICR underlies tLTD, we examined the mechanism responsible for tLTP. We focused on CaMKII as it has been shown to be a link between extracellular calcium and classical LTP in a number of preparations (Lisman et al., 2002). We applied intracellularly 10 μM KN-93, a highly selective CaMKII antagonist, and found that it failed to block tLTD (Fig. 8D; left panel), whose amplitude (76.1 ± 2.8% of control) was similar to that of control conditions (83.2 ± 4% of control; Fig 8E). However, it altered noticeably tLTP amplitude that dropped to 129.4 ± 3.5 % in presence of KN-93 (Fig. 8E), although the difference with tLTP elicited in absence of the drug was not significant ($F_{1, 13}=2.64$, $p = 0.201$).

Role of dopamine receptors

Although data above indicate that cellular mechanisms underlying tLTP and tLTD are markedly different, they provide no evidence whether tLTP and tLTD represent two distinct neuronal populations. To address this question we explored the role of dopamine receptor

agonists as dopamine receptor antagonists had little effects on STDP, presumably because their constitutive basal concentrations was too low in our experimental conditions for the antagonist to have an effect (data not shown). The focus on dopamine receptors stemmed from the fact that in dorsal and ventral striatum, the expression of D1 or D2 receptors is believed to be segregated, with the former expressed in substance P-containing MSNs and the latter in enkephalin-expressing MSNs. This presented the tantalizing possibility that tLTP / tLTD expression in the accumbens could reflect this characteristic.

We measured the effects of D1R and D2R agonists on MSN RMP, Rin, and firing pattern. This last parameter was particularly important as a number of studies showed its sensitivity to dopamine (Akaike et al., 1987; Calabresi et al., 1987). In absence of agonist, we found that all three parameters were very stable over 25 min (Suppl. Fig. 5), assuring that changes observed in presence of the drug could safely be attributed to the drug itself. Following a 30 min period during which we assessed whether the strength of the synaptic transmission of the recorded neuron was increased (tLTP) or weakened (tLTD), we injected hyperpolarizing (−110 pA) and depolarizing (around 260 pA) current pulses (800 ms) every 30 sec for several minutes before exposing the slice to 0.5 μM A-77636, a specific D1R agonist. We measured two markedly different effects of the drug. Figures 9A and B show that in a subset of MSNs A-77636 had no effect on RMP, Rin or firing pattern. In another subset of MSNs, the same agonist profoundly inhibited their firing pattern while leaving their RMP and Rin unchanged (Fig. 9D and E). In these two individual examples, the lack of effects of A-77636 was associated with tLTD cell (Fig. 9C) while inhibition of MSNs excitability was observed in a tLTP-MSN (Fig. 9F). When all tLTD-MSNs were pooled (n = 8), we found that none of the parameters examined (i.e. RMP, Rin, APs number) were affected by drug exposure compared to control conditions (Fig. 10). When all tLTP-MSNs were pooled, we similarly found that neither RMP (Fig. 10A) nor Rin (Fig. 9B) were changed after drug exposure. However, the situation regarding MSNs firing pattern was more complex (Fig. 10C). Thus, as an aggregate (Agre), A-77636 did decrease tLTP-MSNs firing pattern, although this effect was not statistically significant. Separating this group between neurons whose firing pattern was inhibited or not by the drug led us to show that firing pattern of half (n = 4) tLTP-MSNs was totally unaffected (Fig. 10C, “no-Effect”), mirroring results with tLTD-MSNs. However, in the other four tLTP-MSNs, their firing pattern was almost totally inhibited 5–6 min after the beginning of exposure to the D1R agonist (Fig. 10C “Inhibit”).

We tested the effects of 10 μM quinpirole, a selective D2R agonist. Like A-77636, quinpirole had mixed effects. In most cases, MSNs were totally insensitive to quinpirole as illustrated by Fig. 11A and B. In this particular recording, this lack of effects was associated with tLTD (Fig. 11C). In another subset of MSNs, their firing pattern was totally inhibited (Fig. 11D and E). In this neuron, as all other MSNs similarly sensitive to quinpirole, inhibition of firing pattern was not accompanied by a change of RMP or Rin (Fig. 11E), but by a robust tLTP (Fig. 11F). Thus, combining all tLTD-MSNs (n = 6), revealed that quinpirole had no influence on their RMP, Rin or firing pattern (Fig. 12A). A similar approach with tLTP-MSNs revealed that quinpirole had no effects on RMP or Rin (Fig. 12B, left and middle graphs). However, it decreased the number of action potential (Fig. 12B, right panel), although this effect was not statistically significant. This weak effect masked the existence of two subsets of tLTP-MSNs. In a subgroup of 3 tLTP-MSNs, their firing pattern was nearly totally inhibited by quinpirole (Fig. 12C, right graph). In contrast, in 4 out of 7 tLTP-MSNs, quinpirole failed to affect their firing pattern (Fig. 12C, left graph). To our surprise, these data mirrored results obtained with D1 receptor agonist.

Metaplasticity in NAcc MSNs

Although calcium and dopamine data support the notion that tLTP and tLTD occur in different populations of medium spiny neurons, we further explore this idea by pairing AP-

EPSP twice, 10 min apart, using the same delay and frequency (20 ms - 1 Hz). To our surprise, in all (n = 9) MSNs that displayed tLTP following the first induction (121.7 ± 3.6 % of control), not only there was no further potentiation, but synaptic strength was systematically inhibited (or depotentiated) after the second induction (83.4 ± 4.7% of control; Fig. 13A, B and E, gray bars). In contrast, the direction of plasticity in neurons showing tLTD initially remained unchanged, with an inhibition of 90.4 ± 1.7% following the first induction to 80.9 ±11.4 % of control 20 min after the second pairing (n = 4; Fig. 13C, D and E dark bars). This finding further supports the idea that tLTP and tLTD MSNs are not interchangeable and probably occur in neuronal populations with distinct properties. Interestingly, when we changed the pairing order (first AP-EPSP, then EPSP-AP, 20 ms delay at 1 Hz in both conditions), depotentiation was absent (Fig. 13F). Thus, the magnitude of tLTP was the same after the first (145 ± 13.9% of control; n =4) and second induction (145 ± 13.9% of control). Similarly, for tLTD MSNs, we found no change after the second induction compared to the first one (1^{st}: 77.55% and 2^{d}: 76.06% of control).

Discussion

The ability of the same AP-EPSP pairing protocol to induce tLTP and tLTD in NAcc MSNs is a marked departure from brain regions (e.g. CA1 hippocampus and prefrontal cortex) where pairing order determines direction of plasticity (Magee and Johnston, 1997; Markram et al., 1997; Bi and Poo, 1998; Debanne et al., 1998). Because, in these structures, STDP was recorded at excitatory synapses onto glutamatergic neurons, it is more relevant to compare plasticity found at excitatory synapses onto inhibitory neurons, like in accumbens. Thus, in the electric fish cerebellum like structure (Bell et al., 1997), and in dorsal striatum (Fino et al., 2005), tLTP was observed when APs preceded EPSPs. In contrast, reversing the order between APs and EPSPs led to tLTD within a 60-ms window. What accounts for differences between dorsal and ventral (NAcc) striata remains unclear when both regions share many anatomical and functional features. A possible explanation is the modalities of afferents stimulation. Unlike the study by Fino et al (2005), where stimulating electrode was placed in layer V of cerebral cortex, we positioned it in proximity of the recording pipette which likely recruit most glutamatergic afferents (i.e., cortex, hippocampus, and amygdala), not only cortical ones. Therefore, the contribution of each pathway on STDP formation may be different. For example, excitatory inputs of different origins converging onto neighboring dendritic locations of lateral amygdala projection neurons have different forms of plasticity. Inputs from the thalamus readily undergo typical STDP, whereas cortical afferent synapses do not (Huang and Kandel, 1998; Humeau et al., 2003; Humeau et al., 2005). Also, in a recent study in guinea pig, pairing AP with EPSPs evoked simultaneously from cortex and amygdala in conditions close to ours (no GABA antagonist, EPSPs measured at RMP, and pairing frequency of 2 Hz) lead to tLTP but not tLTD (Popescu et al., 2010). Alternatively, dopamine receptors may influence the direction of long-term plasticity as hinted by a recent work in striatum (Shen et al., 2008). Thus, tLTP and tLTD MSNs may express different DARs, on a pattern similar to what is known in dorsal striatum. We tested this idea by evoking STDP (APs-EPSPs, 1 Hz 20 ms) in 16 MSNs in presence of 15 μM sulpiride, a selective dopamine D2R antagonist. We reasoned that if DA is responsible for 50/50 tLTP/tLTD ratio, blocking its receptors may shift this ratio towards tLTP or tLTD. We indeed found such shift from tLTD to tLTP. However, it was only partial as 4 and 12 MSNs underwent tLTD and tLTP, respectively (data not shown). Additionally, tLTD averaged amplitude was larger than in control conditions. This result appears to rule out dopamine receptors as responsible for the difference between ventral and dorsal striatum.

NAcc MSNs tLTP dependence on NMDA receptors is not new and confirms data obtained with HFS-LTP in the same structure (Pennartz et al., 1993; Kombian and Malenka, 1994) as well as in other regions (Lynch et al., 1990). Somewhat more surprising is the apparent lack

of tLTP dependence on CICR. Indeed, since tLTP is independent of APs, calcium dynamics is presumably confined to dendritic spines where small EPSPs evoked NMDA receptor-mediated were shown to release calcium from internal stores (Emptage et al., 1999). Second, a number of studies in hippocampus and ventral striatum appear to support CICR contribution in NMDA receptor-dependent tLTP (Reyes and Stanton, 1996; Wang et al., 1996; Popescu et al., 2010). However, other studies failed to confirm this finding, leaving the exact role of intracellular calcium partially unanswered (Mainen et al., 1999; Kovalchuk et al., 2000). Even more intriguing is the selective dependence of tLTD on action potentials. This contrast with findings from dorsal striatum, and neocortex where pairing EPSPs with subthreshold depolarization evoked a robust tLTD (Sjostrom et al., 2004). Similarly, in dorsal striatum, absence of action potentials does not prevent tLTD formation (Fino et al., 2009), indicating that cellular mechanisms underlying tLTD in accumbens are distinct from other brain regions. The interesting finding is that accumbens tLTD relies on release of intracellular calcium through ryanodine receptors following recruitment of calcium influx through L-type calcium channels, a calcium pathway that is does not appear to underlie tLTP. The role of these high-threshold calcium channels in accumbens mirrors what has been shown in a number of structures including the dorsal striatum (Zhuo and Hawkins, 1995; Choi and Lovinger, 1997; Normann et al., 2000; Kreitzer and Malenka, 2005). However, that of ryanodine receptors is more controversial. Thus, LTD is typically associated with inositol 1,4,5 triphosphate receptors (IP3Rs) in cerebellum and hippocampus (Inoue et al., 1998; Bender et al., 2006), and more importantly in dorsal striatum (Fino et al., 2010). Differences between accumbens and other brain regions regarding the role of ryanodine receptors in tLTD may boil down to characteristics of endoplasmic reticulum. Although ER, which is the single largest intracellular organelle, extends from the nucleus to the dendritic arborization, axon and presynaptic terminals, it is not present homogeneously throughout neurons. Thus, in vivo, ER in hippocampal neurons is found in ~30% of small spines but in the vast majority of large mushroom like spines (Spacek and Harris, 1997). Additionally, in the same neurons, only ryanodine receptors are expressed in spines while both ryanodine and IP3 receptors are found in dendritic ER. It is likely that such a distribution impacts where and how calcium influx control excitability and long-term plasticity. Although there is currently no evidence, distribution of ryanodine receptors in accumbens may be similarly spatially segregated in such a way that only calcium through L-type calcium channels may be in position to induce CICR through ryanodine receptors.

The role of ryanodine receptors is also noteworthy as it may help explain BK channel contribution to accumbens tLTD. Indeed, tLTD may result from the formation of a complex or triad consisting of BK channels, ryanodine receptors and L-type calcium channels. To support this idea, there evidence that neuronal high threshold L-type voltage-gated calcium channels and ryanodine receptors found on membrane of endoplasmic reticulum are in close proximity (Gruol et al., 2010). It is also well established that BK channels and L-type form large protein complex (Marrion and Tavalin, 1998; Sun et al., 2003; Marcantoni et al., 2010). Finally, in cerebellar granule cells, Chavis et al (1998) reported that both L-type VGCC and ryanodine receptors regulate BK channels activity. Taken together, these data strongly support the view that these three channels are likely located in very close proximity to each other, regulating calcium dynamics in discrete portion of plasmalemma membrane (nanodomain), an ideal configuration for regulating plasticity in core accumbens medium spiny neurons.

Effects of dopamine receptor agonists on action potential patterns were somewhat surprising. First, we found that only a quarter of all MSNs were sensitive to the drugs. Second, A-77636 and quinpirole had similar effects on MSNs spiking. Finally, there was no relationship between D1 / D2R expression on the one hand and tLTP/LTD on the other. The ability of both D1R and D2R agonists to increase MSN excitability appears to contradict

early studies showing that although D1 class receptors reduced spike activity evoked by current injection in both dorsal and ventral striatum (Akaike et al., 1987; Calabresi et al., 1987) presumably through their action on voltage-gated Na^+ and K^+ channels (Surmeier et al., 1992; Surmeier et al., 1995; Hernandez_Lopez et al., 1997), D2R agonists had the opposite effects (Akaike et al., 1987). However, more recent studies shed new light on regulation of MSNs excitability by D2Rs. Thus, Surmeier et al (1992) reported that D2Rs could either enhance or inhibit sodium channels (see also Surmeier 2007). It is interesting to note that in our study, inhibition of tLTP-MSN excitability was not accompanied by a change of resting membrane potential. We only observed a steady hyperpolarization of about 2 mV in only one MSN, which rules out anomalous rectifying K^+ channels that regulate RMP, as shown by Pacheco-Cano (1996). In keeping with previous studies (Surmeier et al., 1992; Hernandez_Lopez et al., 1997; Salgado et al., 2005), Na^+ and/or Ca^{++} channels are more likely to mediate dopamine receptors' effects on MSNs excitability. Although from our data we cannot infer whether D1Rs and D2Rs are expressed in the same tLTP-MSNs that represent about 25% of all neurons tested, anatomical data appear to support this idea. Although early studies suggested that D1 and D2Rs were largely segregated in dorsal striatum (Gerfen et al., 1990) and nucleus accumbens (Le Moine and Bloch, 1996; Lu et al., 1998; Schwartz et al., 1998), other studies have nuanced this idea. Thus, a single cell rt-PCR study was the first one to demonstrate that a substantial number of MSNs (~ 25%) in dorsal striatum expressed both D1Rs and D2Rs, a conclusion supported to an even greater degree by the work of Aizman et al (2000). Although D1R/D2R coexpression in the accumbens has not been established, it is likely that these receptors also coexist in this region.

Although MSNs, which represent nearly 90% of all accumbens neurons, are typically treated as an homogenous population, there is anatomical and chemical heterogeneity within this structure (Meredith and Totterdell, 1999; Zhou et al., 2003). However, functionally, such heterogeneity has never fully translated to synaptic plasticity. The present data provide evidence that all spiny neurons are not created equal in their ability to undergo plasticity. This tLTP/tLTD dichotomy may represent the first degree of functional framework that may help tease out the various functions associated with accumbens. Indeed, if this region is mostly studied for its role in drug addiction, it is also involved in feeding, pain, and depression (Altier and Stewart, 1999; Salamone et al., 2005; Baldo and Kelley, 2007), pathologies that may be controlled by very different subsets of MSNs. Nevertheless, further studies are needed to establish unequivocally whether tLTP and tLTD MSNs are really two distinct populations. A key experiment will be to examine similarities/differences of mRNAs coding for various channels and receptors using single cell rt-PCR.

Supplementary Material

Refer to Web version on PubMed Central for supplementary material.

Acknowledgments

This work was supported by the National Institutes of Alcohol Abuse and Alcoholism (NIAAA) and the Integrative Neuroscience Initiative on Alcohol Abuse (INIA).

Abbreviations

APs	action potentials
CaMKII	calcium-calmoduline Kinase II
CICR	calcium-induced calcium release

fAHP	fast afterhyperpolarization
Rin	input resistance
LTD	long-term depression
LTP	long-term potentiation
RMP	resting membrane potential
STDP	spike-timing dependent plasticity
EPSCs	spontaneous Excitatory Postsynaptic Current

Bibliography

Aizman O, Brismar H, Uhlen P, Zettergren E, Levey AI, Forssberg H, Greengard P, Aperia A. Anatomical and physiological evidence for D1 and D2 dopamine receptor colocalization in neostriatal neurons. Nat Neurosci. 2000; 3:226–230. [PubMed: 10700253]

Akaike A, Ohno Y, Sasa M, Takaori S. Excitatory and inhibitory effects of dopamine on neuronal activity of the caudate nucleus neurons in vitro. Brain Res. 1987; 418:262–272. [PubMed: 2890403]

Altier N, Stewart J. The role of dopamine in the nucleus accumbens in analgesia. Life Sci. 1999; 65:2269–2287. [PubMed: 10597883]

Baldo BA, Kelley AE. Discrete neurochemical coding of distinguishable motivational processes: insights from nucleus accumbens control of feeding. Psychopharmacology (Berl). 2007; 191:439–459. [PubMed: 17318502]

Behrens R, Nolting A, Reimann F, Schwarz M, Waldschutz R, Pongs O. hKCNMB3 and hKCNMB4, cloning and characterization of two members of the large-conductance calcium-activated potassium channel beta subunit family. FEBS Lett. 2000; 474:99–106. [PubMed: 10828459]

Bell CC, Han VZ, Sugawara Y, Grant K. Synaptic plasticity in a cerebellum-like structure depends on temporal order. Nature. 1997; 387:278–281. [PubMed: 9153391]

Bender VA, Bender KJ, Brasier DJ, Feldman DE. Two coincidence detectors for spike timing-dependent plasticity in somatosensory cortex. J Neurosci. 2006; 26:4166–4177. [PubMed: 16624937]

Bi GQ, Poo MM. Synaptic modifications in cultured hippocampal neurons: dependence on spike timing, synaptic strength, and postsynaptic cell type. J Neurosci. 1998; 18:10464–10472. [PubMed: 9852584]

Bliss TV, Collingridge GL. A synaptic model of memory: long-term potentiation in the hippocampus. Nature. 1993; 361:31–39. [PubMed: 8421494]

Bliss TV, Lømo T. Long-lasting potentiation of synaptic transmission in the dentate area of the anaesthetized rabbit following stimulation of the perforant path. J Physiol. 1973; 232:331–356. [PubMed: 4727084]

Calabresi P, Mercuri N, Stanzione P, Stefani A, Bernardi G. Intracellular studies on the dopamine-induced firing inhibition of neostriatal neurons in vitro: evidence for D1 receptor involvement. Neuroscience. 1987; 20:757–771. [PubMed: 2955246]

Caporale N, Dan Y. Spike timing-dependent plasticity: a hebbian learning rule. Annu Rev Neurosci. 2008; 31:25–46. [PubMed: 18275283]

Carelli RM, Ijames SG. Nucleus accumbens cell firing during maintenance, extinction, and reinstatement of cocaine self-administration behavior in rats. Brain Res. 2000; 866:44–54. [PubMed: 10825479]

Chavis P, Ango F, Michel JM, Bockaert J, Fagni L. Modulation of big K+ channel activity by ryanodine receptors and L-type Ca2+ channels in neurons. Eur J Neurosci. 1998; 10:2322–2327. [PubMed: 9749760]

Chen BT, Hopf FW, Bonci A. Synaptic plasticity in the mesolimbic system: therapeutic implications for substance abuse. Ann N Y Acad Sci. 2010; 1187:129–139. [PubMed: 20201850]

Choi S, Lovinger DM. Decreased probability of neurotransmitter release underlies striatal long-term depression and postnatal development of corticostriatal synapses. Proc Natl Acad Sci U S A. 1997; 94:2665–2670. [PubMed: 9122253]

Debanne D, Gahwiler BH, Thompson SM. Long-term synaptic plasticity between pairs of individual CA3 pyramidal cells in rat hippocampal slice cultures. J Physiol. 1998; 507:237–247. [PubMed: 9490845]

Emptage N, Bliss TV, Fine A. Single synaptic events evoke NMDA receptor-mediated release of calcium from internal stores in hippocampal dendritic spines. Neuron. 1999; 22:115–124. [PubMed: 10027294]

Fino E, Deniau JM, Venance L. Brief subthreshold events can act as Hebbian signals for long-term plasticity. PLoS One. 2009; 4:e6557. [PubMed: 19675683]

Fino E, Glowinski J, Venance L. Bidirectional activity-dependent plasticity at corticostriatal synapses. J Neurosci. 2005; 25:11279–11287. [PubMed: 16339023]

Fino E, Paille V, Cui Y, Morera-Herreras T, Deniau JM, Venance L. Distinct coincidence detectors govern the corticostriatal spike timing-dependent plasticity. J Physiol. 2010

Gerfen CR, Engber TM, Mahan LC, Susel Z, Chase TN, Monsma FJJ, Sibley DR. D1 and D2 dopamine receptor-regulated gene expression of striatonigral and striatopallidal neurons. Science. 1990; 250:1429–1432. [PubMed: 2147780]

Grueter BA, Brasnjo G, Malenka RC. Postsynaptic TRPV1 triggers cell type-specific long-term depression in the nucleus accumbens. Nat Neurosci. 2010; 13:1519–1525. [PubMed: 21076424]

Gruol DL, Netzeband JG, Nelson TE. Somatic Ca2+ signaling in cerebellar Purkinje neurons. J Neurosci Res. 2010; 88:275–289. [PubMed: 19681168]

Hernandez_Lopez S, Bargas J, Surmeier DJ, Reyes A, Galarraga E. D1 receptor activation enhances evoked discharge in neostriatal medium spiny neurons by modulating an L-type Ca2+ conductance. J Neurosci. 1997; 17:3334–3342. [PubMed: 9096166]

Hollander JA, Ijames SG, Roop RG, Carelli RM. An examination of nucleus accumbens cell firing during extinction and reinstatement of water reinforcement behavior in rats. Brain Res. 2002; 929:226–235. [PubMed: 11864628]

Huang YY, Kandel ER. Postsynaptic induction and PKA-dependent expression of LTP in the lateral amygdala. Neuron. 1998; 21:169–178. [PubMed: 9697861]

Humeau Y, Herry C, Kemp N, Shaban H, Fourcaudot E, Bissiere S, Luthi A. Dendritic spine heterogeneity determines afferent-specific Hebbian plasticity in the amygdala. Neuron. 2005; 45:119–131. [PubMed: 15629707]

Humeau Y, Shaban H, Bissiere S, Luthi A. Presynaptic induction of heterosynaptic associative plasticity in the mammalian brain. Nature. 2003; 426:841–845. [PubMed: 14685239]

Hyman SE, Malenka RC, Nestler EJ. Neural mechanisms of addiction: the role of reward-related learning and memory. Annu Rev Neurosci. 2006; 29:565–598. [PubMed: 16776597]

Inoue T, Kato K, Kohda K, Mikoshiba K. Type 1 inositol 1,4,5-trisphosphate receptor is required for induction of long-term depression in cerebellar Purkinje neurons. J Neurosci. 1998; 18:5366–5373. [PubMed: 9651219]

Kauer JA, Malenka RC. Synaptic plasticity and addiction. Nat Rev Neurosci. 2007; 8:844–858. [PubMed: 17948030]

Kombian SB, Malenka RC. Simultaneous LTP of non-NMDA- and LTD of NMDA-receptor-mediated responses in the nucleus accumbens. Nature. 1994; 368:242–246. [PubMed: 7908412]

Kovalchuk Y, Eilers J, Lisman J, Konnerth A. NMDA receptor-mediated subthreshold Ca(2+) signals in spines of hippocampal neurons. J Neurosci. 2000; 20:1791–1799. [PubMed: 10684880]

Krause M, German PW, Taha SA, Fields HL. A pause in nucleus accumbens neuron firing is required to initiate and maintain feeding. J Neurosci. 2010; 30:4746–4756. [PubMed: 20357125]

Kreitzer AC, Malenka RC. Dopamine modulation of state-dependent endocannabinoid release and long-term depression in the striatum. J Neurosci. 2005; 25:10537–10545. [PubMed: 16280591]

Le Moine C, Bloch B. Expression of the D3 dopamine receptor in peptidergic neurons of the nucleus accumbens: comparison with the D1 and D2 dopamine receptors. Neuroscience. 1996; 73:131–143. [PubMed: 8783237]

Lisman J, Schulman H, Cline H. The molecular basis of CaMKII function in synaptic and behavioural memory. Nat Rev Neurosci. 2002; 3:175–190. [PubMed: 11994750]

Lu XY, Ghasemzadeh MB, Kalivas PW. Expression of D1 receptor, D2 receptor, substance P and enkephalin messenger RNAs in the neurons projecting from the nucleus accumbens. Neuroscience. 1998; 82:767–780. [PubMed: 9483534]

Lynch G, Kessler M, Arai A, Larson J. The nature and causes of hippocampal long-term potentiation. Prog Brain Res. 1990; 83:233–250. [PubMed: 2168058]

Magee JC, Johnston D. A synaptically controlled, associative signal for Hebbian plasticity in hippocampal neurons. Science. 1997; 275:209–213. [PubMed: 8985013]

Mainen ZF, Malinow R, Svoboda K. Synaptic calcium transients in single spines indicate that NMDA receptors are not saturated. Nature. 1999; 399:151–155. [PubMed: 10335844]

Marcantoni A, Vandael DH, Mahapatra S, Carabelli V, Sinnegger-Brauns MJ, Striessnig J, Carbone E. Loss of Cav1.3 channels reveals the critical role of L-type and BK channel coupling in pacemaking mouse adrenal chromaffin cells. J Neurosci. 2010; 30:491–504. [PubMed: 20071512]

Margrie TW, Brecht M, Sakmann B. In vivo, low-resistance, whole-cell recordings from neurons in the anaesthetized and awake mammalian brain. Pflugers Arch. 2002; 444:491–498. [PubMed: 12136268]

Markram H, Lubke J, Frotscher M, Sakmann B. Regulation of synaptic efficacy by coincidence of postsynaptic APs and EPSPs. Science. 1997; 275:213–215. [PubMed: 8985014]

Marrion NV, Tavalin SJ. Selective activation of Ca2+-activated K+ channels by co-localized Ca2+ channels in hippocampal neurons. Nature. 1998; 395:900–905. [PubMed: 9804423]

Martin G, Puig S, Pietrzykowski A, Zadek P, Emery P, Treistman S. Somatic localization of a specific large-conductance calcium-activated potassium channel subtype controls compartmentalized ethanol sensitivity in the nucleus accumbens. J Neurosci. 2004; 24:6563–6572. [PubMed: 15269268]

Matthews EA, Weible AP, Shah S, Disterhoft JF. The BK-mediated fAHP is modulated by learning a hippocampus-dependent task. Proc Natl Acad Sci U S A. 2008; 105:15154–15159. [PubMed: 18799739]

Meredith GE, Totterdell S. Microcircuits in nucleus accumbens' shell and core involved in cognition and reward. Psychobiology. 1999; 27:165–186.

Miranda P, de la Pena P, Gomez-Varela D, Barros F. Role of BK potassium channels shaping action potentials and the associated [Ca(2+)](i) oscillations in GH(3) rat anterior pituitary cells. Neuroendocrinology. 2003; 77:162–176. [PubMed: 12673050]

Normann C, Peckys D, Schulze CH, Walden J, Jonas P, Bischofberger J. Associative long-term depression in the hippocampus is dependent on postsynaptic N-type Ca2+ channels. J Neurosci. 2000; 20:8290–8297. [PubMed: 11069935]

Pacheco-Cano MT, Bargas J, Hernandez-Lopez S, Tapia D, Galarraga E. Inhibitory action of dopamine involves a subthreshold Cs(+)-sensitive conductance in neostriatal neurons. Exp Brain Res. 1996; 110:205–211. [PubMed: 8836685]

Pennartz CM, Ameerun RF, Groenewegen HJ, Lopes da Silva FH. Synaptic plasticity in an in vitro slice preparation of the rat nucleus accumbens. Eur J Neurosci. 1993; 5:107–117. [PubMed: 7903183]

Poolos NP, Johnston D. Calcium-activated potassium conductances contribute to action potential repolarization at the soma but not the dendrites of hippocampal CA1 pyramidal neurons. J Neurosci. 1999; 19:5205–5212. [PubMed: 10377332]

Popescu AT, Saghyan AA, Nagy FZ, Pare D. Facilitation of corticostriatal plasticity by the amygdala requires Ca2+-induced Ca2+ release in the ventral striatum. J Neurophysiol. 2010; 104:1673–1680. [PubMed: 20554836]

Puig MV, Celada P, Diaz-Mataix L, Artigas F. In vivo modulation of the activity of pyramidal neurons in the rat medial prefrontal cortex by 5-HT2A receptors: relationship to thalamocortical afferents. Cereb Cortex. 2003; 13:870–882. [PubMed: 12853374]

Reyes M, Stanton PK. Induction of hippocampal long-term depression requires release of Ca2+ from separate presynaptic and postsynaptic intracellular stores. J Neurosci. 1996; 16:5951–5960. [PubMed: 8815877]

Robbe D, Alonso G, Manzoni OJ. Exogenous and endogenous cannabinoids control synaptic transmission in mice nucleus accumbens. Ann N Y Acad Sci. 2003; 1003:212–225. [PubMed: 14684448]

Robbe D, Bockaert J, Manzoni OJ. Metabotropic glutamate receptor 2/3-dependent long-term depression in the nucleus accumbens is blocked in morphine withdrawn mice. Eur J Neurosci. 2002a; 16:2231–2235. [PubMed: 12473091]

Robbe D, Alonso G, Duchamp F, Bockaert J, Manzoni OJ. Localization and mechanisms of action of cannabinoid receptors at the glutamatergic synapses of the mouse nucleus accumbens. J Neurosci. 2001; 21:109–116. [PubMed: 11150326]

Robbe D, Kopf M, Remaury A, Bockaert J, Manzoni OJ. Endogenous cannabinoids mediate long-term synaptic depression in the nucleus accumbens. Proc Natl Acad Sci U S A. 2002b; 99:8384–8388. [PubMed: 12060781]

Rosenkranz JA, Grace AA. Modulation of basolateral amygdala neuronal firing and afferent drive by dopamine receptor activation in vivo. J Neurosci. 1999; 19:11027–11039. [PubMed: 10594083]

Salamone JD, Correa M, Mingote SM, Weber SM. Beyond the reward hypothesis: alternative functions of nucleus accumbens dopamine. Curr Opin Pharmacol. 2005; 5:34–41. [PubMed: 15661623]

Salgado H, Tecuapetla F, Perez-Rosello T, Perez-Burgos A, Perez-Garci E, Galarraga E, Bargas J. A reconfiguration of CaV2 Ca2+ channel current and its dopaminergic D2 modulation in developing neostriatal neurons. J Neurophysiol. 2005; 94:3771–3787. [PubMed: 16120665]

Schramm NL, Egli RE, Winder DG. LTP in the mouse nucleus accumbens is developmentally regulated. Synapse. 2002; 45:213–219. [PubMed: 12125042]

Schwartz JC, Diaz J, Bordet R, Griffon N, Perachon S, Pilon C, Ridray S, Sokoloff P. Functional implications of multiple dopamine receptor subtypes: the D1/D3 receptor coexistence. Brain Res Brain Res Rev. 1998; 26:236–242. [PubMed: 9651537]

Shen W, Flajolet M, Greengard P, Surmeier DJ. Dichotomous dopaminergic control of striatal synaptic plasticity. Science. 2008; 321:848–851. [PubMed: 18687967]

Sjostrom PJ, Rancz EA, Roth A, Hausser M. Dendritic excitability and synaptic plasticity. Physiol Rev. 2008; 88:769–840. [PubMed: 18391179]

Sjostrom PJ, Turrigiano GG, Nelson SB. Endocannabinoid-dependent neocortical layer-5 LTD in the absence of postsynaptic spiking. J Neurophysiol. 2004; 92:3338–3343. [PubMed: 15240760]

Spacek J, Harris KM. Three-dimensional organization of smooth endoplasmic reticulum in hippocampal CA1 dendrites and dendritic spines of the immature and mature rat. J Neurosci. 1997; 17:190–203. [PubMed: 8987748]

Sun X, Gu XQ, Haddad GG. Calcium influx via L- and N-type calcium channels activates a transient large-conductance Ca2+-activated K+ current in mouse neocortical pyramidal neurons. J Neurosci. 2003; 23:3639–3648. [PubMed: 12736335]

Surmeier DJ, Bargas J, Hemmings HCJ, Nairn AC, Greengard P. Modulation of calcium currents by a D1 dopaminergic protein kinase/phosphatase cascade in rat neostriatal neurons. Neuron. 1995; 14:385–397. [PubMed: 7531987]

Surmeier DJ, Ding J, Day M, Wang Z, Shen W. D1 and D2 dopamine-receptor modulation of striatal glutamatergic signaling in striatal medium spiny neurons. Trends Neurosci. 2007; 30:228–235. [PubMed: 17408758]

Surmeier DJ, Eberwine J, Wilson CJ, Cao Y, Stefani A, Kitai ST. Dopamine receptor subtypes colocalize in rat striatonigral neurons. Proc Natl Acad Sci U S A. 1992; 89:10178–10182. [PubMed: 1332033]

Thomas MJ, Malenka RC, Bonci A. Modulation of long-term depression by dopamine in the mesolimbic system. J Neurosci. 2000; 20:5581–5586. [PubMed: 10908594]

Van der Kloot W. The regulation of quantal size. Prog Neurobiol. 1991; 36:93–130. [PubMed: 1847748]

Wang Y, Wu J, Rowan MJ, Anwyl R. Ryanodine produces a low frequency stimulation-induced NMDA receptor-independent long-term potentiation in the rat dentate gyrus in vitro. J Physiol. 1996; 495:755–767. [PubMed: 8887781]

Yaka R, Phamluong K, Ron D. Scaffolding of Fyn kinase to the NMDA receptor determines brain region sensitivity to ethanol. J Neurosci. 2003; 23:3623–3632. [PubMed: 12736333]

Zhou L, Furuta T, Kaneko T. Chemical organization of projection neurons in the rat accumbens nucleus and olfactory tubercle. Neuroscience. 2003; 120:783–798. [PubMed: 12895518]

Zhuo M, Hawkins RD. Long-term depression: a learning-related type of synaptic plasticity in the mammalian central nervous system. Rev Neurosci. 1995; 6:259–277. [PubMed: 8717637]

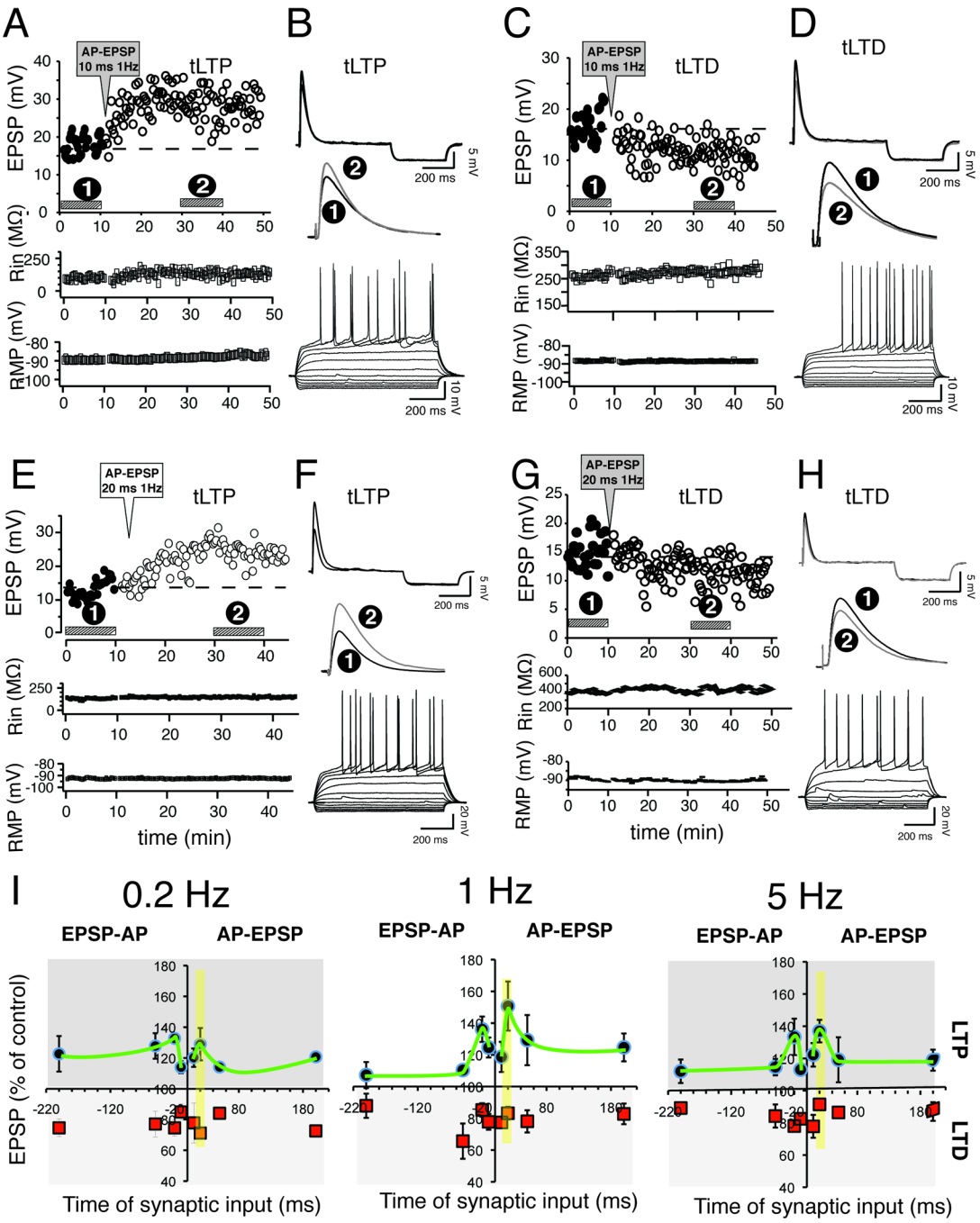

Figure 1. The same AP-EPSP pairing conditions evoke both tLTP *and* tLTD

A Graph of EPSP amplitude monitored every 20 sec before (control, solid dots) and after (tLTP, open dots) induction (AP-EPSP, 10 ms 1Hz). Horizontal bars indicate where EPSPs were recorded to obtain averaged traces shown in B (top and middle). Membrane input resistance (middle graph) and resting membrane potential (lower graph) were similarly monitored every 20 sec. **B** Averaged (30 traces) EPSPs from control conditions (dark line) and 20 min after induction (grey line). Downward traces following EPSPs are hyperpolarizing potentials in response to short negative current steps to monitor input resistance. Middle panel shows enlarged averaged EPSPs. Bottom panel, current-voltage

relationship from the same cell shows all the characteristics of a MSN. **C** and **D** panels: tLTD in another MSN using the same parameters as in A. Panels **E** and **F**; and **G** and **H**. tLTP and tLTD, respectively, in two different MSNs when AP-EPSP delay was increased to 20 ms. **I** Averaged EPSP amplitudes expressed as percent of control in various experimental conditions where the frequency of AP-EPSP and EPSP-AP pairings varies from 0.2 (left), 1 (middle), and to 5 Hz (right graph). Red and black symbols represent tLTD and tLTP, respectively. The delay between the two electrical events (x axis), is noted as negative when the EPSP precedes the AP, and positive when it follows (right half of each graph). The green line is not an actual fit, simply a visual aid. Between 9 and 16 MSNs were tested in each experimental condition.

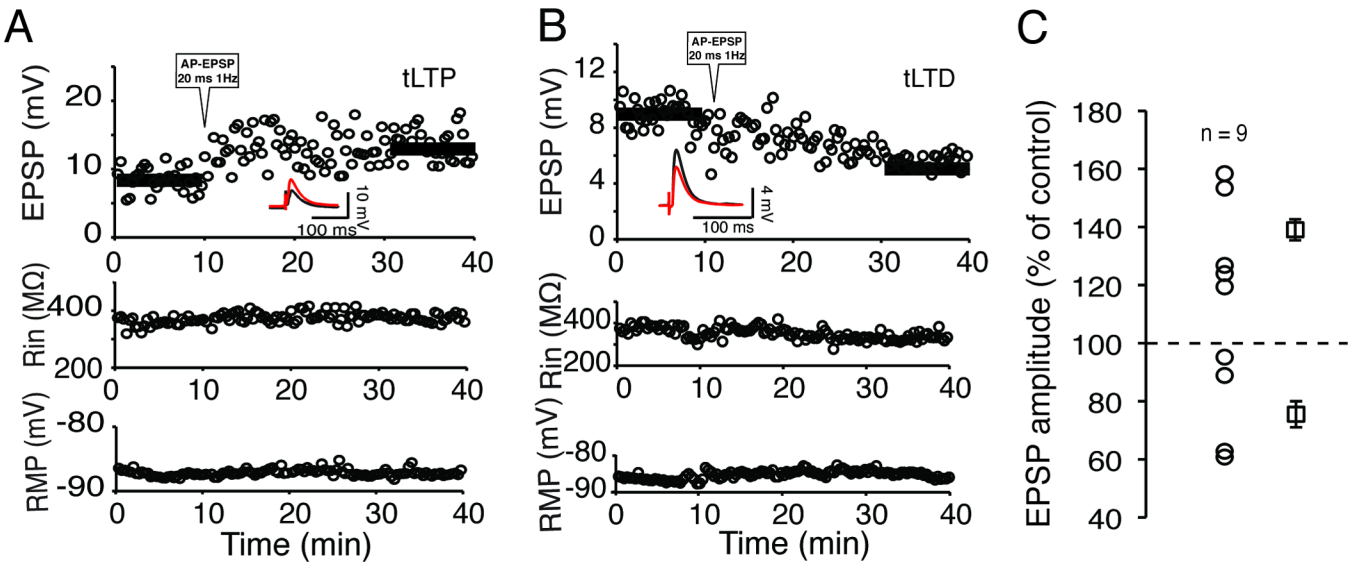

Figure 2. $GABA_A$ receptor antagonist does not affect STDP

A graph of EPSP amplitude, from a MSN, monitored very 20 sec for 40 min, showing tLTP in presence of 15 μM bicuculline. The pairing protocol (AP-EPSP, 20 ms 1 Hz) was applied following a 10 min control period. Solid horizontal bars indicate average EPSP amplitudes before and after the first pairings. Two lower panels show input resistance (Rin) and RMP over the same recording period. **B** Same graph as in A form another MSN showing tLTD. **C** Averaged EPSP amplitudes expressed as percent of control in presence of bicuculline. Each symbol represents a MSN. Symbols on the right with S.E.M show averaged tLTP and tLTD amplitude.

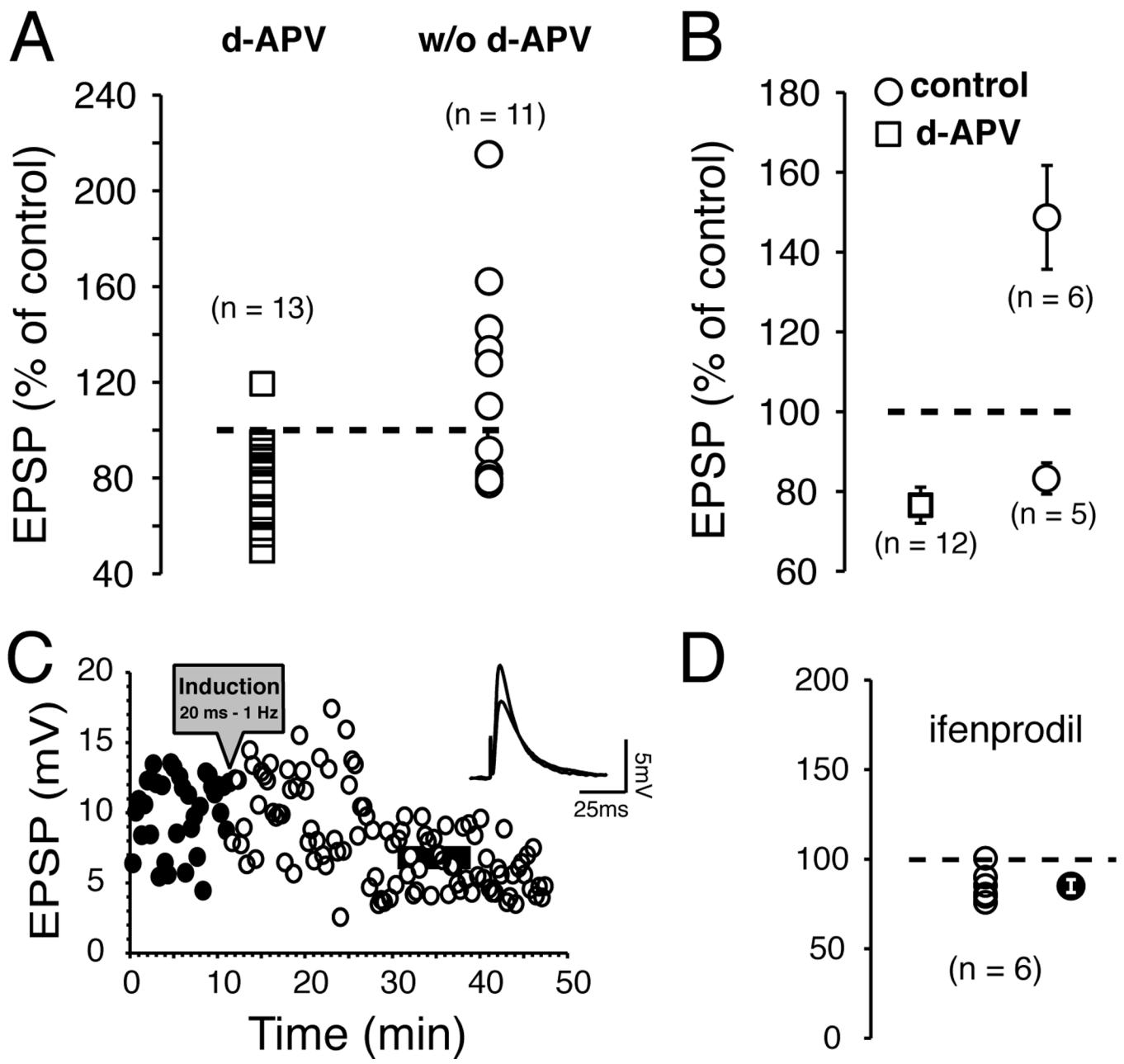

Figure 3. tLTP, but not tLTD, is NMDA receptor-dependent

A Graph of EPSP amplitude changes measured 20 min after induction. Circles and square symbols represent changes of MSN EPSP amplitude measured 20 min after induction in presence (d-APV) or absence (w/o d-APV) of d-APV in wt mice, respectively. Changes are expressed in percent of control (broken line). Symbols above broken line show tLTP, while those below show tLTD. **B** Average amplitude of tLTP and tLTD in presence (open squares) and absence (control, open circles) of d-APV. **C** Representative example of EPSPs amplitude depression after induction (black circles). EPSPs were monitored every 20 sec for up to 50 min. Dark and grey lines of inset indicate the averaged amplitude of 30 consecutive EPSPs recorded over a period of 10 min before and 20 min after induction, respectively. **D** Graph of EPSP amplitude changes 20 min after induction in presence 10 μM ifenprodil. Each open symbol shows an individual MSN. Averaged change is indicated by filled circle.

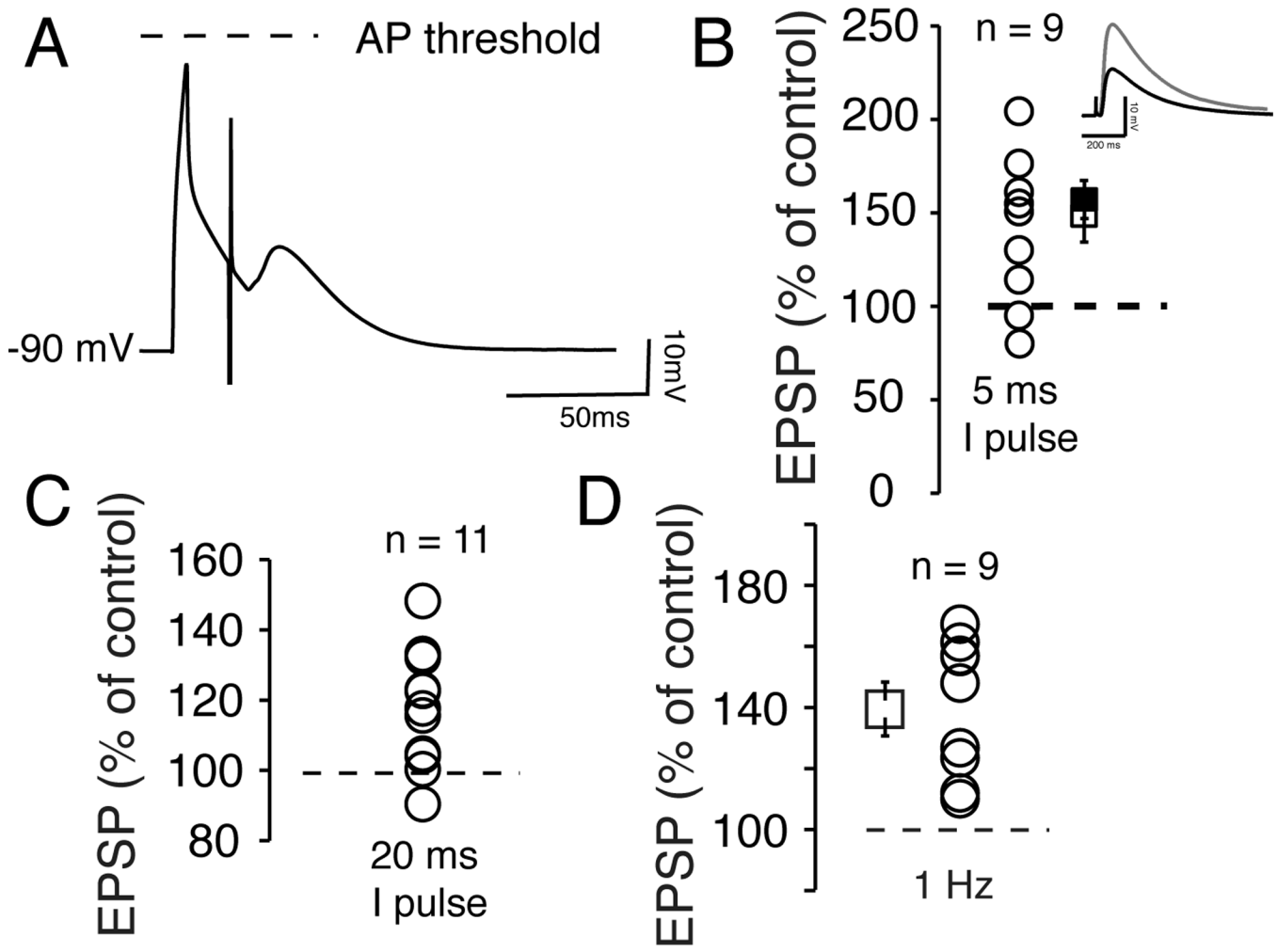

Figure 4. APs control tLTD, but not tLTP, in NAcc MSNs

A Representative trace of a brief subthreshold depolarization paired with an EPSP with a 20 ms delay. Broken line indicates AP threshold. **B** Changes of EPSP amplitude measured 20 min after induction, expressed in percent of control (indicated with the broken line) in 9 MSNs. Symbols show average tLTP in presence (open square) and absence (solid square) of APs during pairing. Inset shows averaged amplitude of 30 EPSPs of a representative MSN undergoing tLTP, measured before (dark trace) and after induction (grey traces). **C** Effect of a longer depolarizing current pulse on EPSP amplitude in 11 MSNs. **D** EPSP amplitude in 9 MSNs, expressed as percent of control, after stimulation frequency was increased to 1 Hz (no AP was paired with EPSP during induction).

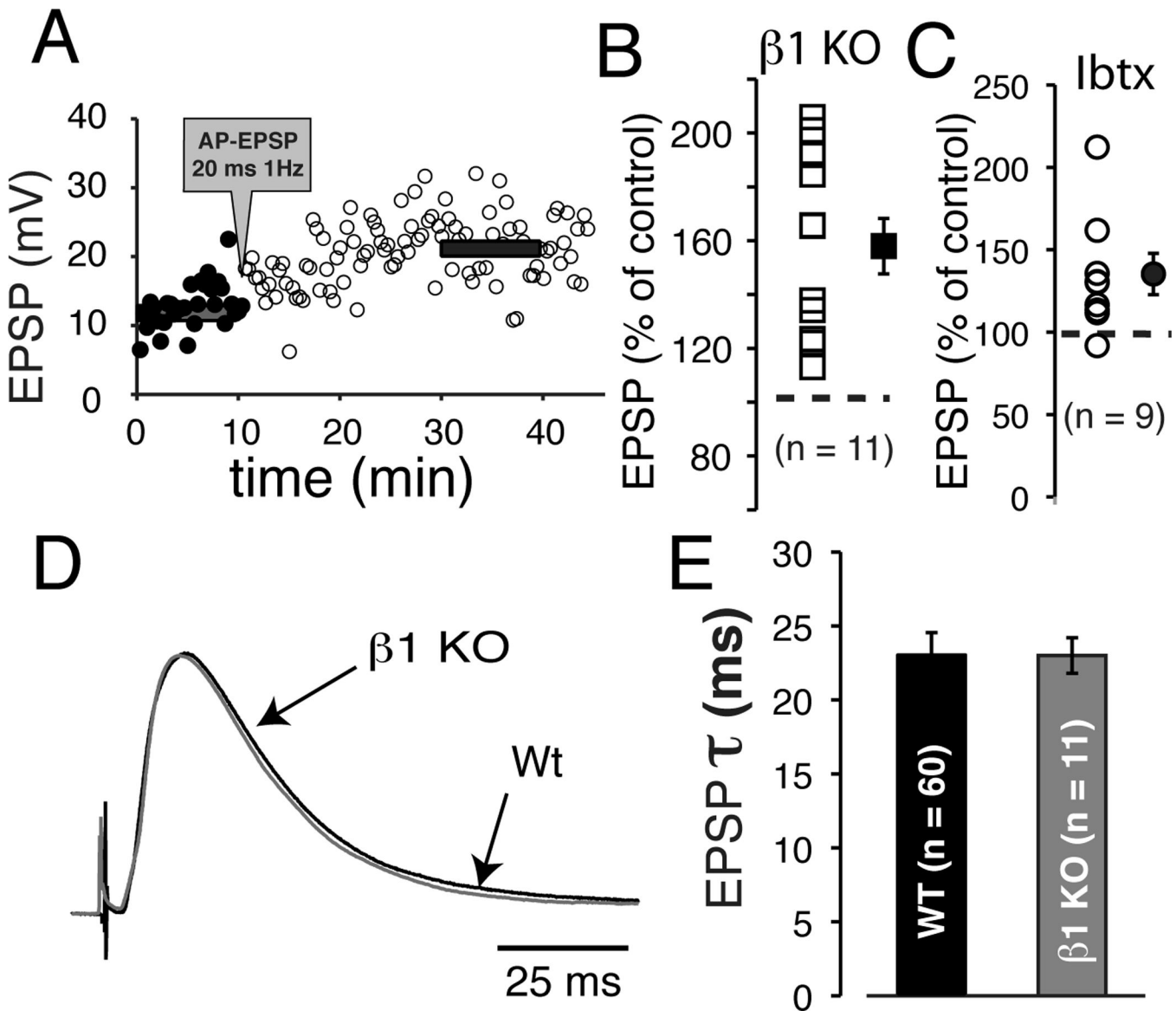

Figure 5. Alteration of AP properties inhibits tLTD

A Representative graph of a MSN EPSP amplitude monitored every 20 sec for 45 min in a β1 KO mouse. Horizontal bars indicate average EPSP amplitudes before and 20 min after pairing. **B** Averaged EPSP amplitude after induction in β1 KO mouse. **C** Averaged EPSP amplitude after induction in slices exposed to 1 μM Iberiotoxin. **D** Representative EPSPs recorded in wt (black trace), and β1 KO mice (gray trace, KO mice). Traces were recorded before induction and are the average of 30 consecutive EPSPs evoked every 20 sec. **F** Averaged EPSP tau values (in ms) in wild type (wt, black column), and β1 KO mice (light gray column).

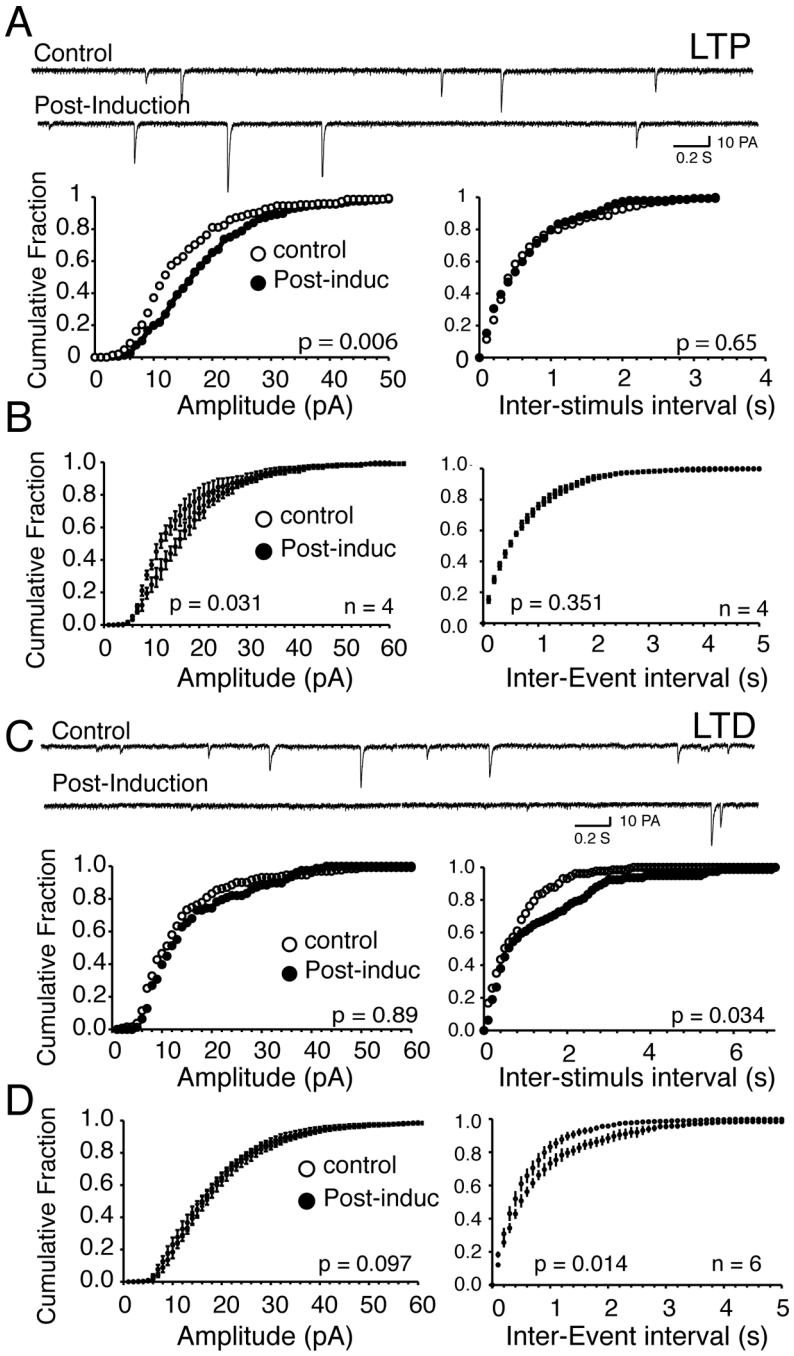

Figure 6. tLTD but not tLTP is associated with a decrease of glutamate release

A Traces of sEPSCs measured at resting membrane potentials (−91 mV) from a representative NAcc MSN before (control) and 15 min after (post-induction) tTLP induction. Each downward deflection represents one sEPSC. Lower panels show cumulative fraction amplitude (left panel) and frequency histograms (right panel) of same neuron. **B** Averaged cumulative fraction histograms of spontaneous EPSCs amplitude (left panel) and frequency (right panel) in tLTP MSNs (n = 4). While inter-event interval shifts to the right (i.e. lower frequency) after induction in tLTD MSNs only, there is not change of amplitude. **C** Traces of sEPSCs measured at resting membrane potentials (−88 mV) from another

representative NAcc MSN before (control) and 15 min after (post-induction) tTLD induction. Lower panels show cumulative fraction histogram of amplitude (left panel) and frequency (right panel) of same neuron. **D** Averaged cumulative fraction histograms of sEPSCs amplitude (left panel) and frequency (right panel) in tLTD MSNs (n = 6). Statistical comparison before and after induction is shown in lower right corner of each histogram.

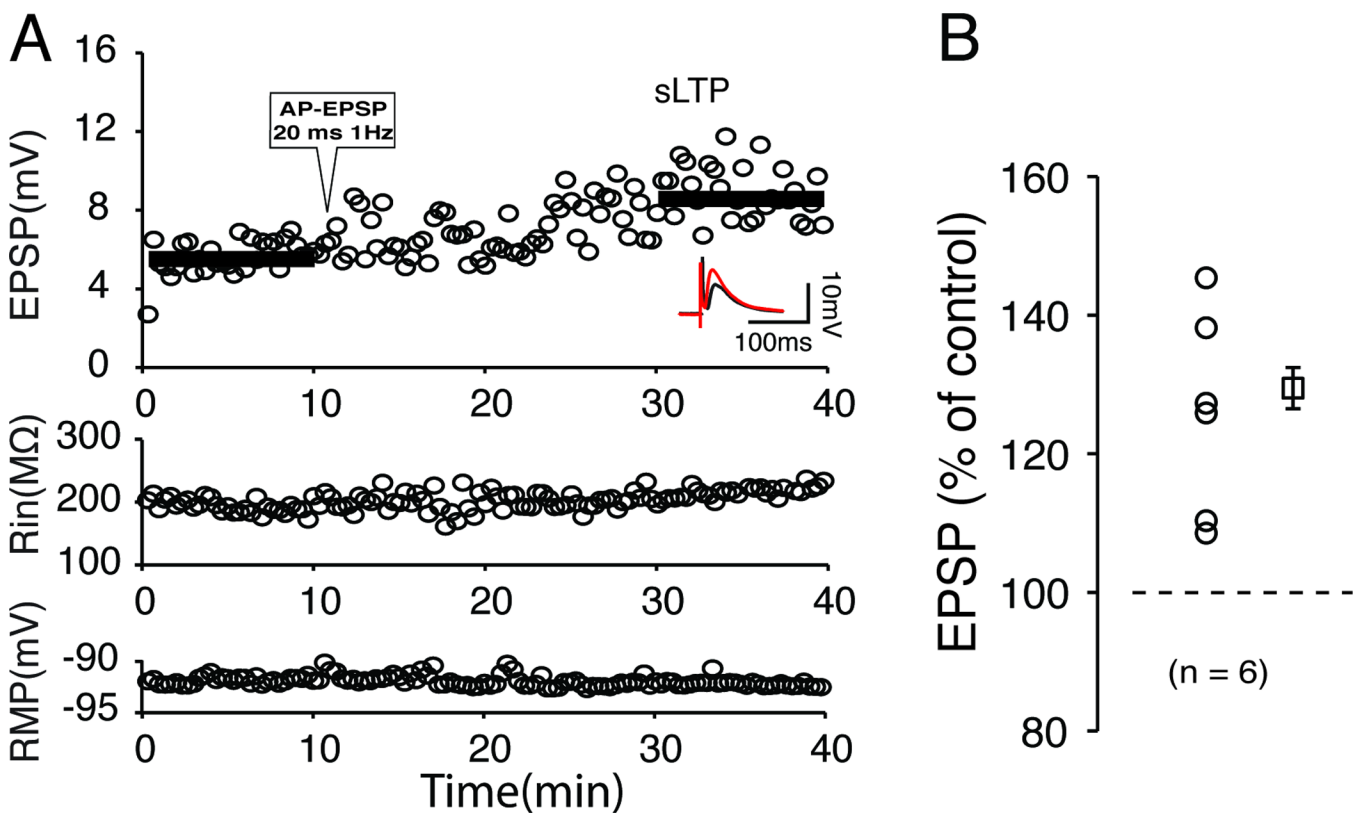

Figure 7. Endocannabinoid receptor 1 antagonist AM-251 (2 μM) blocks tLTD but not tLTP

A EPSP amplitude monitored every 20 sec before and after induction (AP-EPSP 20 ms 1 Hz) of a representative MSN. Middle and bottom panels show resting potential (RMP) and input resistance (Rin) of the same neuron. **B** EPSP amplitude measured 20 min after induction expressed as percent of control. Square symbol shows the averaged EPSP amplitude after induction.

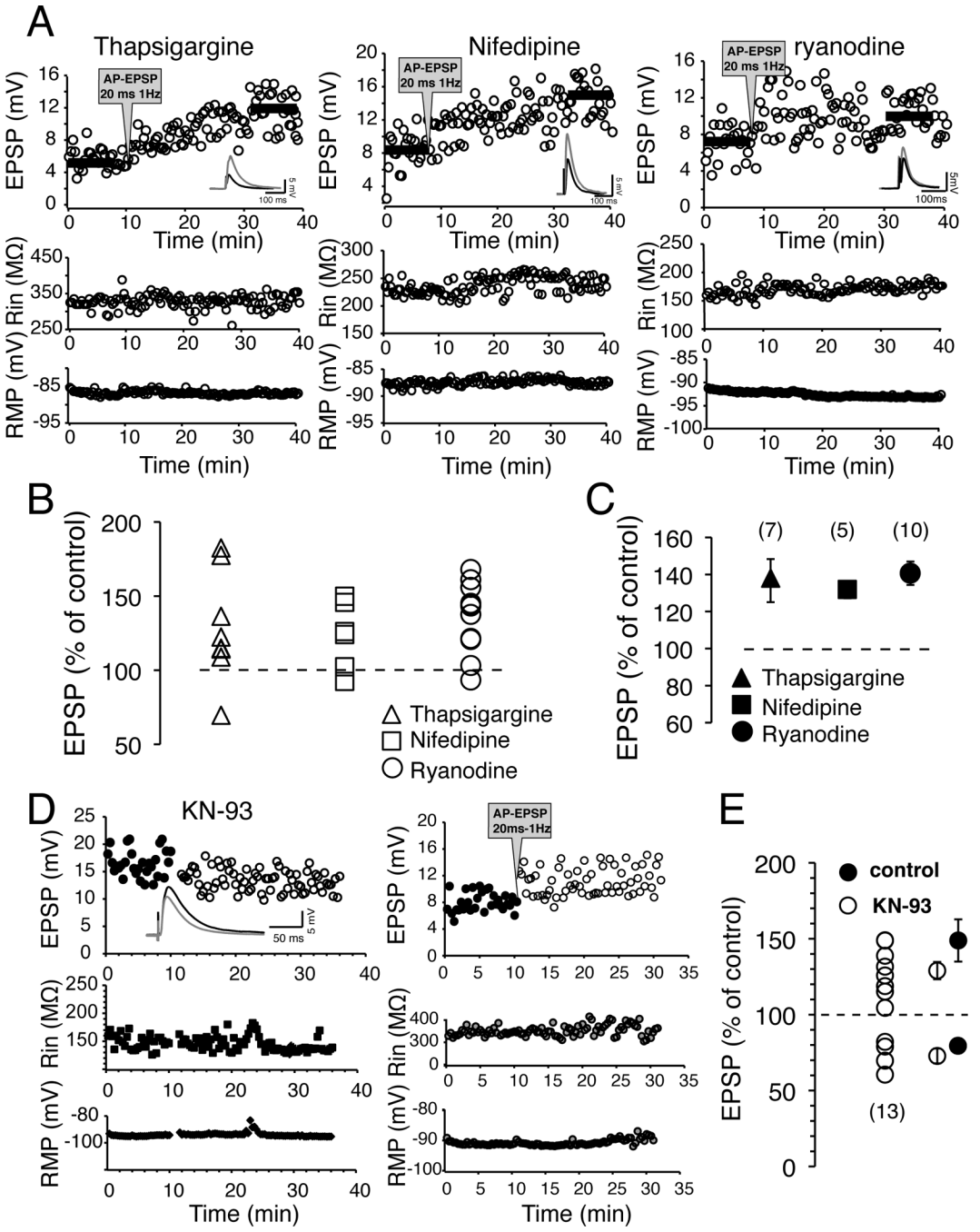

Figure 8. High threshold calcium channels and calcium-induced calcium release underlie tLTD but not tLTP

A Representative example of effects of 5 μM thapsigargine, 5 μM nifedipine and 10 μM ryanodine on MSNs plasticity. Top panels show EPSP amplitude measured every 20 sec before and after induction. Dark horizontal bars show where amplitude of averaged EPSPs was measured. Middle and Bottom panels show input resistance and RMP throughout recordings. **B** Effects of tharpsigargine (triangles), nifedipine (squares) and ryanodine (circles) on MSNs plasticity. Symbols above broken line indicate tLTP. Note that only one or two MSNs undergo tLTD in all experimental conditions. **C** Averaged effects of the drugs on MSNs plasticity. Values are expressed as % of control ± SEM. **D** Representative tLTD

(left panel) and tLTP (right panel) in presence of 10 μM KN-93 in recording pipette. **E** Effects of 10 μM KN-93 on long-term plasticity of 13 MSNs. Averaged effects on STDP, in presence (KN-93; open symbols) and absence (control; solid symbols) of the drug, are shown as % of control ± SEM.

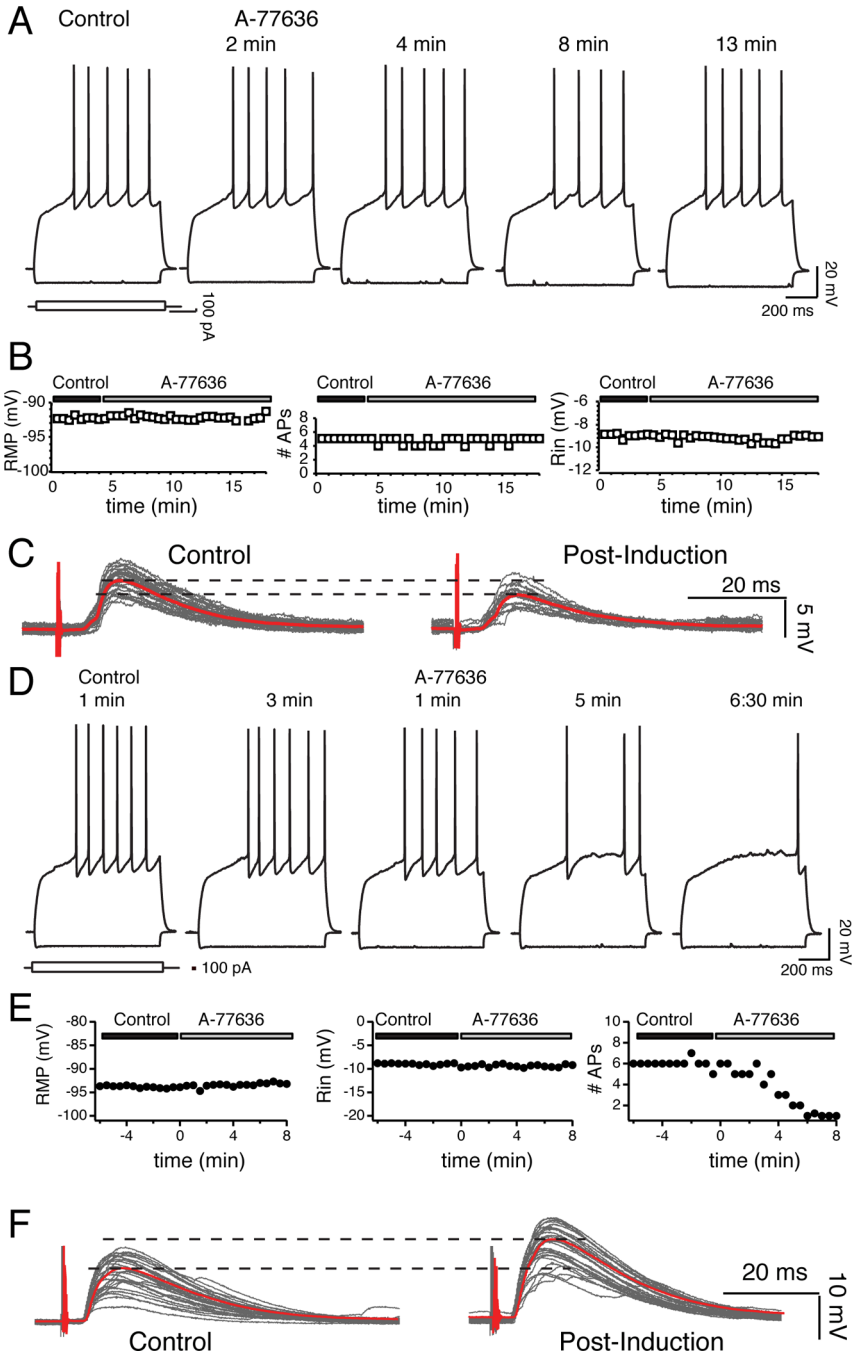

Figure 9. Differential effects of D1 receptor agonist A-77636 on tLTP- and tLTD-MSNs

A Voltage traces in response to hyperpolarizing (−110 pA) and depolarizing (+260 pA) current pulses (800 ms) recorded at various interval before (control) and during exposure to A-77636 (A-77636). Note A77636's lack of effects on the neuron resting membrane potential, input resistance, and spiking. **B** Graphs of resting membrane potential (left panel, input resistance (expressed as amplitude of voltage deflection in mV, middle panel), and number of action potentials (right panel) of neuron shown in A, monitored every 30 sec before and during exposure to the drug. Again, note the stability of all three parameters during the recording session. **C** EPSPs traces measured every 20 sec at RMP before

(control) and after AP-EPSP pairing (post-induction) from same neuron shown in A. The red lines represent cumulative EPSPs traces in control and post-induction conditions. **D** Voltage traces of a difference MSN in response to hyperpolarizing (−110 pA) and depolarizing (+270 pA) current pulses recorded at various interval before (control) and during exposure to A-77636 (A-77636). Note the massive effect of the drug on spike firing. **E** Graphs of resting membrane potential (left panel, input resistance (middle panel), and number of action potentials (right panel) monitored every 30 sec before and during exposure to the drug. Note the strong inhibition of this neuron firing rate that drops to near zero 5 min after drug exposure, while its RMP and Rin remain stable. **F** EPSPs traces measured every 20 sec at RMP before (control) and after AP-EPSP pairing (post-induction) from neuron shown in D. The red lines represent cumulative EPSPs traces in control and post-induction conditions.

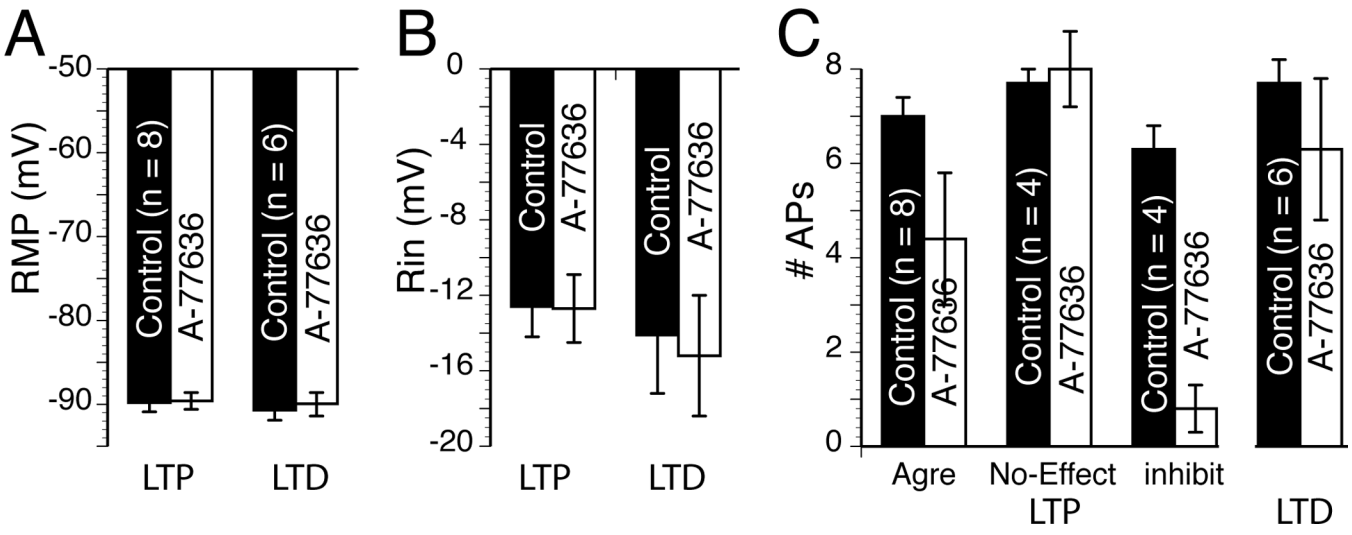

Figure 10. D1R agonist fails to alter tLTD- but inhibits tLTP-MSNs firing pattern

A Graph shows resting membrane potential measured before (control) and during A-77636 exposure (A-77636) in tLTP- (n = 8) and tLTD-MSNs (n = 6). **B** Graph of averaged input resistance expressed as amplitude of hyperpolarizing voltage deflection in response to −110 pA current pulses in tLTP- and tLTD-MSNs. **C** Averaged number of action potentials measured before and during drug exposure. We agregated all tLTP-MSNs (agre) before grouping them based on the sensitivity of their firing pattern to A-77636 (inhibit) or not (no-effect). All values were expressed as averaged ± SEM.

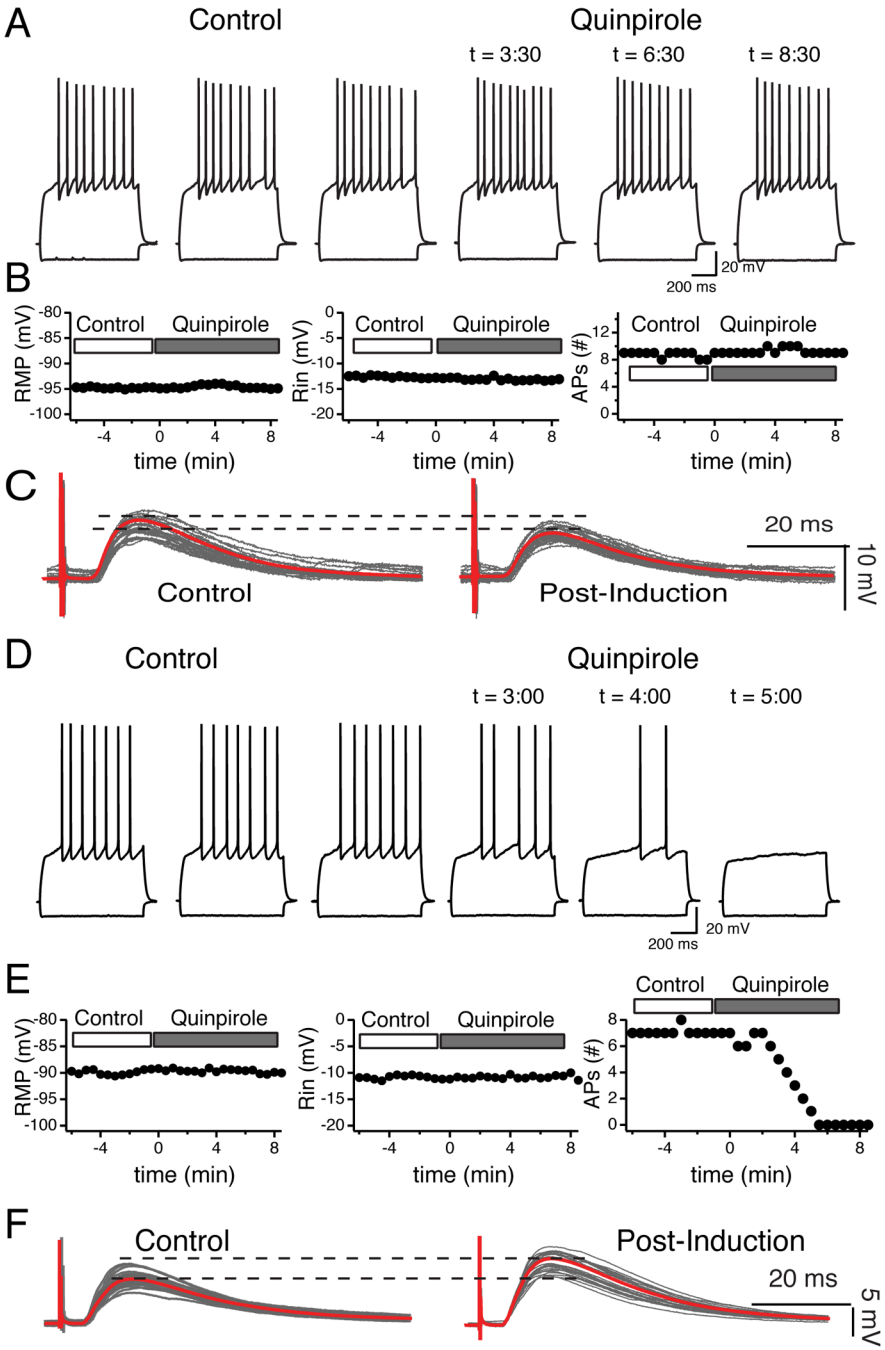

Figure 11. D2 receptor agonist quinpirole affects tLTP- but not tLTD-MSNs

A Voltage traces in response to hyperpolarizing (−110 pA) and depolarizing (+250 pA) current pulses (800 ms) recorded at various time points before (control) and during exposure to quinpirole (quinpirole). Note quinpirole's lack of effects on the neuron resting membrane potential, input resistance, and spiking. **B** From cell shown in panel A, graphs of resting membrane potential (left panel, input resistance (expressed as amplitude of voltage deflection in mV, middle panel), and number of action potentials (right panel) monitored every 30 sec before and during exposure to the drug. Again, note the stability of all three parameters during the recording session. **C** EPSPs traces measured every 20 sec at RMP

before (control) and after AP-EPSP pairing (post-induction) from same neuron shown in A. The red lines represent cumulative EPSPs traces in control and post-induction conditions. **D** Voltage traces of a difference MSN in response to hyperpolarizing (−110 pA) and depolarizing (+280 pA) current pulses recorded at various interval before (control) and during exposure to quinpirole. Note the massive effect of the drug on spike firing. **E** Graphs of resting membrane potential (left panel), input resistance (middle panel), and number of action potentials (right panel) monitored every 30 sec before and during exposure to the drug. Note the strong inhibition of this neuron firing rate that drops to zero 5 min after drug exposure, while its RMP and Rin remain stable. **F** EPSPs traces measured every 20 sec at RMP before (control) and after AP-EPSP pairing (post-induction) from neuron shown in D. The red lines represent cumulative EPSPs traces in control and post-induction conditions.

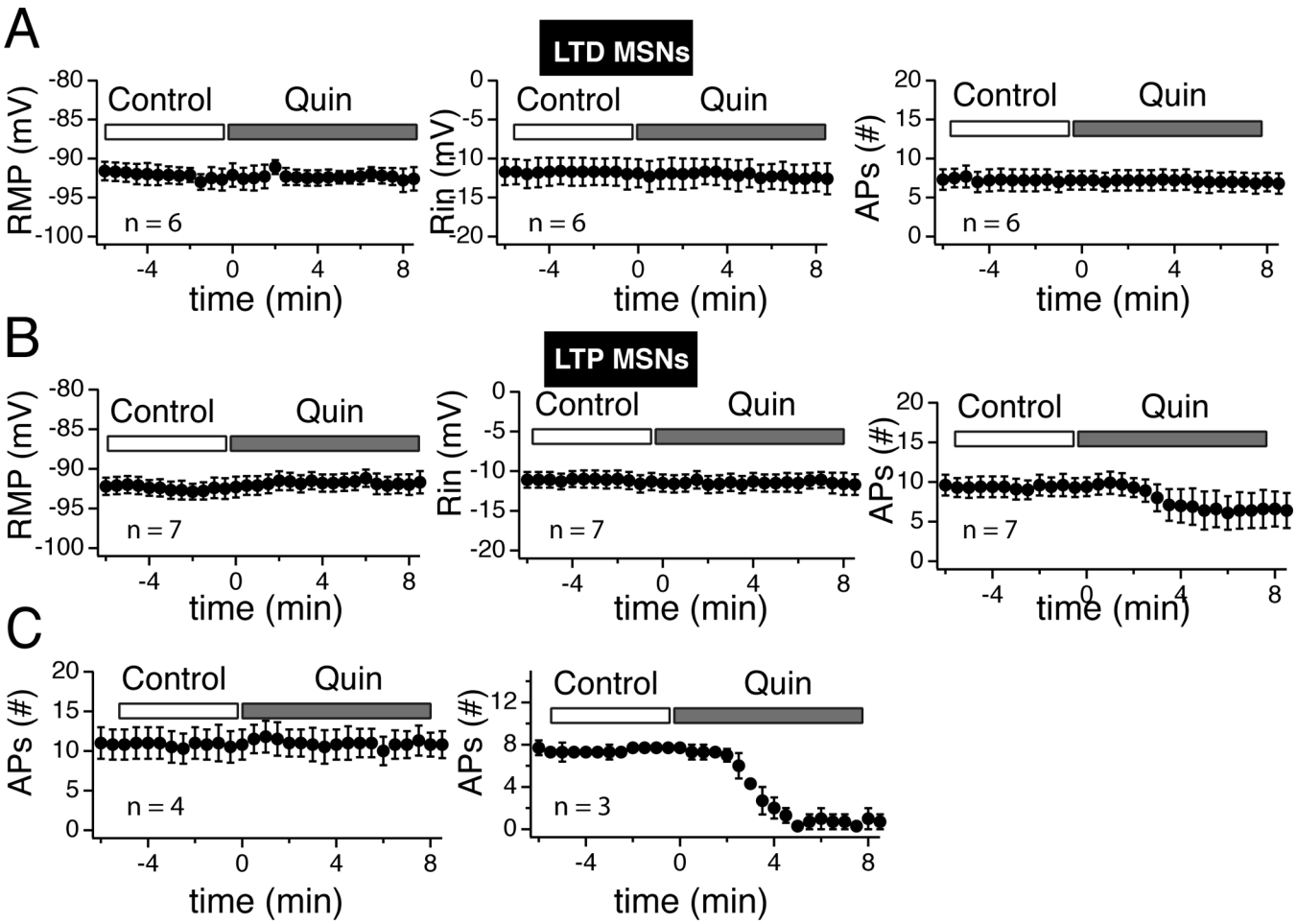

Figure 12. Quinpirole failed to alter tLTD- but inhibited tLTP-MSNs

A Averaged values of RMP (left panel), Rin (middle panel), and number of action potentials (right panel) monitored every 30 sec before (control) and during quinpirole (Quin) exposure in tLTD-MSNs (n = 6). Note the stability of all parameters. **B** Graphs show the same parameters (RMP, Rin, #APs) in tLTP-MSNs (n = 7). Contrary to tLTD neurons, there is a noticeable decrease of the number of APs (right panel). **C** tLTP-MSNs shown in previous panel have been split based on their response to quinpirole. Left graph groups tLTP-MSNs showing no sensitivity to the drug. Right panel shows the number of action potentials from the subset of tLTP neurons (n = 3) whose firing patterns were inhibited by quinpirole.

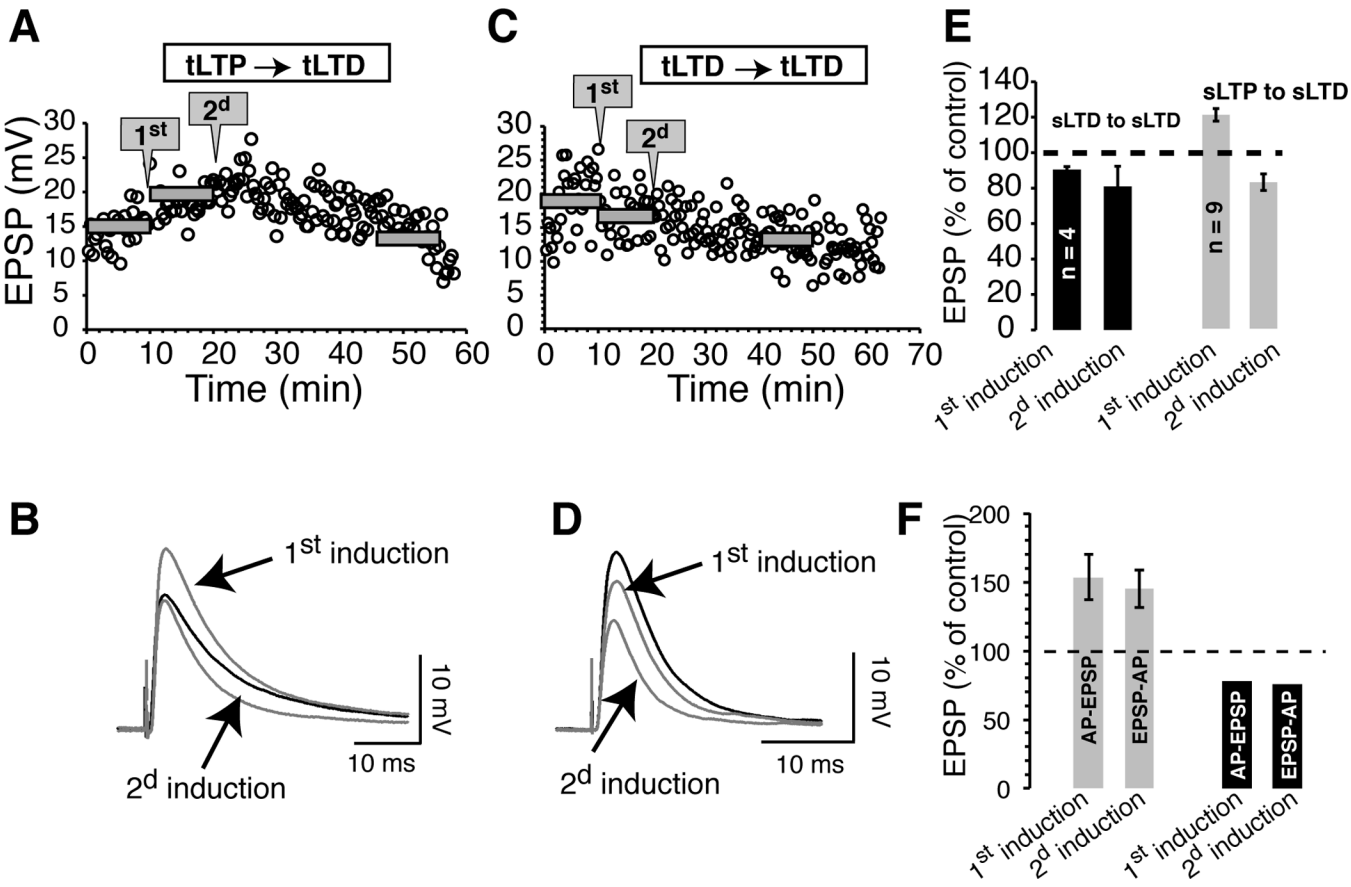

Figure 13. Metaplasticity in tLTP, but not tLTD MSNs

A graph of EPSP amplitude, from a MSN, monitored very 20 sec for nearly one hour. The same pairing protocol (AP-EPSP, 20 ms 1 Hz) was applied twice with an interval of 10 min (gray arrowed-boxes). Gray horizontal bars indicate average EPSP amplitudes before and after the first and second pairings. **B** averaged (30 traces) EPSPs in control (dark line) conditions and after first and second induction (gray traces). **C** Same protocol as in A in a cell initially showing tLTD. **D** averaged (30 traces) EPSPs from control (dark line) conditions and after first and second induction (gray traces). **E** averaged effects of the first and second induction on EPSP amplitude. The change following the second pairing is expressed as a control of EPSP amplitude measured after the first pairing. **F** averaged effects of the first and second induction on EPSP amplitude. The pairing order between the first and second induction was reversed from AP-EPSP to EPSP-AP (20 ms, 1 Hz). Solid bars indicate averaged EPSP amplitude over 10 min periods.

Table 1

Changes in EPSP amplitude, expressed as percent of control, in various experimental conditions. Frequencies are indicated above table. The order of the AP/EPSP pairing is shown in the red boxes, while delay between these two electrical events is shown on the left. The number of neurons recorded is indicated next to each tLTP and tLTD columns.

	0.2 Hz				1 Hz				5 Hz			
AP-EPSP	**tLTP**	**n**	**tLTD**	**n**	**tLTP**	**n**	**tLTD**	**n**	**tLTP**	**n**	**tLTD**	**n**
10	122.2 ± 7.3	6	77.8 ± 7.1	3	118.7 ± 9.5	4	77.4 ± 3.3	4	120.2 ± 6	7	77.8 ± 13	4
20	136.9 + 7	6	91.4 ± 1.9	5	148.7 ± 15.5	6	83.2 ± 4	5	129 ± 10.5	4	71.2 ± 3.1	7
50	119.1 ± 14	3	86.4 ± 3.3	5	129.3 ± 15.8	5	78.1 ± 7	11	114.1 ± 0.9	5	84.1 ± 2.1	11
200	118.9 ± 6.5	6	87 ± 5.8	6	124.7 ± 8.8	6	82.8 ± 6.5	9	120.7 ± 2.9	3	72.6 ± 3.3	9
EPSP-AP	**tLTP**	**n**	**tLTD**	**n**	**tLTP**	**n**	**tLTD**	**n**	**tLTP**	**n**	**tLTD**	**n**
−10	113 ± 3.7	9	82.5	2	124.6 ± 6.3	6	77.8 ± 5	5	114 ± 3.9	6	84.9 ± 5.2	5
−20	133.3 ± 11.3	6	78 ± 3.3	6	136.1 ± 8	7	85.3 ± 4.2	9	132.7	2	74.6 ± 5.3	9
−50	114.6 ± 5.1	3	84.2 ± 7.2	9	110.4 ± 3.5	5	65.6 ± 11.1	5	127.8 ± 8.3	4	77.1 ± 8.4	5
−200	112 ± 7.3	3	89.2 ± 3.6	8	107.3 ± 8.2	4	87.9 ± 7.6	9	122.7 ± 11.5	4	74.6 ± 5.8	9